MethodsX 14 (2025) 103200

Contents lists available at ScienceDirect

MethodsX

journal homepage: www.elsevier.com/locate/methodsx

Microplastics and nanoplastics detection using flow cytometry: Challenges and methodological advances with fluorescent dye application

Lucas Ainé[a,b], Justine Jacquin[a], Colette Breysse[a], Catherine Colin[a], Jean-Michel Andanson[b], Florence Delor-Jestin[b,*]

[a] CT-IPC: CT-IPC 3 rue Emile Duclaux, Biopôle Clermont, Limagne, 63360 SAINT-BEAUZIRE
[b] Université Clermont Auvergne, Clermont Auvergne INP, CNRS, ICCF, F-63000 Clermont–Ferrand, France

REVIEW HIGHLIGHTS

- Flow cytometry coupled with Nile Red analysis has recently been applied to micro and nano plastics quantification.
- A detailed overview of this emerging method, its advantages and its remaining obstacles to be addressed are discussed.
- The key areas for improving the method's robustness, along with suggestions for future developments, are provided.

ARTICLE INFO

Keywords:
Microplastic
Nanoplastic
Nile red
Flow cytometry

ABSTRACT

Flow cytometry (FC) enables the precise quantification of specific types of microparticles and larger nanoparticles (>200 nm) in liquid media. Initially developed for biological applications, this technique has recently been adapted to the environmental field for the measurement of microplastics and nanoplastics (MNPs). Nile Red, a fluorochrome extensively used in MNP analysis due to its effectiveness and accessibility, has been applied to significantly enhance the sensitivity and specificity of MNP detection of this technique. Additionally, flow cytometry offers the advantage of automated detection, allowing the quantification of smaller particles, including those under 1 µm, which are often missed by traditional spectroscopic methods. However, despite its promise, the presence of undissolved dye in aqueous media presents a significant challenge for accurate quantification. In recent years, various methodologies have been developed to overcome these limitations, including the use of co-solvents, surfactants, and pre-filtration or pre-sonication techniques to enhance quantification accuracy. This review examines recent literature on MNPs detection via FC, with a focus on technical improvements made and the remaining metrological challenges, offering insights into how this method can be further refined for future investigations.

Specifications table

Subject area:	Environmental ScienceEnvironmental Science
More specific subject area:	Microplastics and nanoplastics quantification
Name of the reviewed methodology:	Flow Cytometry coupled with Nile Red staining for microplastics and nanoplastics quantification
Keywords:	Microplastics; Nanoplastics; Flow Cytometry; Nile Red

* Corresponding author.
E-mail addresses: Lucas.AINE@ct-ipc.com (L. Ainé), Justine.JACQUIN@ct-ipc.com (J. Jacquin), Colette.BREYSSE@ct-ipc.com (C. Breysse), Catherine.COLIN@ct-ipc.com (C. Colin), j-michel.andanson@uca.fr (J.-M. Andanson), florence.delor_jestin@sigma-clermont.fr (F. Delor-Jestin).

https://doi.org/10.1016/j.mex.2025.103200
Received 14 November 2024; Accepted 3 February 2025
Available online 4 February 2025

(continued on next page)

Resource availability:	
Review question:	What are key steps to consider when using this method?
	What are the main issues to consider and be cautious of?
	What are the main and most relevant improvement solutions that have been implemented so far?
	What are the potential avenues for improvement in future work?

Background

The growing interest in accurately quantifying microplastics is well-established, and many researchers have repurposed their existing equipment for this type of analysis due to both expertise and economic considerations. Originally from the biological field, flow cytometry has been recently adapted (2020) for environmental applications to measure microplastics and nanoplastics, using Nile Red staining to improve detection sensitivity and specificity. Since then, a total of nine articles have been published and its significant advantages suggest that more will be published in the coming years. Indeed, this emerging technique holds significant promises.

First, it leverages the Nile Red fluorochrome, which has been extensively used in microplastic quantification due to its effectiveness, affordability, and compatibility with labs equipped with fluorescence microscopes. Then, beyond its technical advantages, this method also enables automated detection and quantification of smaller microplastics than those typically measured by vibrational spectroscopy techniques, which struggle to detect particles between 1 and 20 μm. In fact, it can even identify submicron particles. Finally, flow cytometry is relatively easy to use.

However, several published papers on the topic are overwhelmingly positive and often overlook inherent limitations. Indeed, several metrological issues need to be addressed for a comprehensive evaluation of this method. Two main issues have been spotted on this technique. The Nile Red precipitates in aqueous medias, inherent to flow cytometry. This results in the formation of aggregates that may fluoresce, potentially causing false positives. The second issue concerns data treatment. False positives and background noise overlapping with microplastics signals are significant sources of bias. The aim of this review is to outline the advancements made in the field to provide guidance on their correct application to microplastics. It first fully explains flow cytometry analysis and its recent application to microplastics with Nile Red staining, with a brief history of the technique and details needed to better understand the advantages and the issue. It then exposes the issues and the development that have been performed to answer them.

This review not only highlights these challenges and limitations, but also explores existing solutions and potential future developments to improve the accuracy of microplastics quantification. It aims to provide researchers interested in testing this method on microplastics with critical insights, offering recommendations on how to avoid pitfalls and enhance the methodology.

Method details

Introduction

Microplastics and nanoplastics (MNPs) have been thoroughly investigated over the past decade due to their potential impact on health and the environment. They have been detected in significant quantities in almost every medium, including various environmental settings and living organisms [37], alerting us to the impact they could have on living beings. The amount of MNPs in the oceans alone is estimated to be >15 million tons [33] or from 15 to 51 trillion pieces of plastic [51]. Environmental studies have highlighted their extensive dispersion. MNPs have been found in oceans, rivers, lakes, soil, air, and even polar regions, illustrating their pervasive nature and underscoring the need for comprehensive monitoring. The exposition to MNPs has been associated with changes in behaviour, metabolism, and development, demonstrating notable toxicity that influences the immune system, induces DNA oxidation, and causes damage to cell tissues and the neuronal system. Nanoplastics (NPs), and microplastics (MPs) smaller than 20 μm are of greater concern due to their physical properties [60] and their ability to penetrate biological barriers [18,24,31,43]. They have been detected in several human tissues like the placenta (5 to 10 μm) [56] and lung tissues [2]. A review by Laura Schröter and Natascia Ventura on the toxicological impacts of NPs highlighted their significant toxicity across various biological systems [59]. They noted that MNPs smaller than the pore size of the affected organ tend to accumulate more readily. However, despite those conclusions, NP analysis remains challenging in terms of robustness and reliability. This lack of precise measurement tools for NPs hinders our ability to evaluate their environmental distribution and potential risks comprehensively. Addressing this methodological limitation is crucial for improving the assessment of MNP exposure and guiding regulatory frameworks. Given the widespread dispersion and significant toxicity of small MPs and NPs, their abundance, and their enhanced ability to reach biological organs, precise measurement of NPs across various environmental media is crucial. However, conventional spectroscopic methods like Fourier-transform infrared spectroscopy (FTIR) and Raman spectroscopy, which are widely used for identifying MPs, are effective for particles larger than 10–20 μm for FTIR and down to about 1 μm for Raman spectroscopy [53]. Despite their effectiveness, these methods require refinement in data processing and analysis [54]. They can also be time-consuming, and variation can still be observed depending on the laboratory or method used [53]. While those conventional methods are effective for detecting MPs down to 1 μm, there is still a significant lack of methodology for accurately measuring particles smaller than this size [39]. The World Health Organization has called for standardized methods to improve the reliability of data [77]. Therefore, developing simpler and faster methods for measuring MNPs, especially NPs, is essential to better understand and mitigate their health and environmental risks. Recently, Qian

Table 1
Characteristics of synthetic MNPs and experimental samples, along with their corresponding organic pre-treatment done on natural samples tested by FC coupled with NR. /: no digestion performed.

Reference	Synthetic used MNPs for calibration samples	Experimental media analysed	Organic Pre-treatment
[35]	Scratched pieces of PS, PE, PET, HDPE, LDPE, PVC, PP, PA, and PC	None	/
[71]	(1, 10 and 38 μm) PS microspheres, LDPE, PP, PMMA, PVC, PLA and ABS synthetic irregularly shaped MPs' solutions at 400, 4000 and 40,000 particle/mL	Coastal marine water	H_2O_2 30 %, 5 h, 70 °C
[57]	(0.2, 0.5 and 0.8 μm) microspheres, *nature of polymer not specified*	Human peripheral blood (adults and new-borns)	1 % aqueous potassium hydroxide (KOH), at least 10 days, 60 °C
[70]	(1, 4, 6, 10, 15 and 38 μm) PS microspheres	Bottled and tap water	/
[7]	(0.6, 0.7, 1, 2, 3, 4, 5, 6, 10 and 15 μm) PS microspheres, (< 25 μm) PS, (740–4990 nm) PE, (3 μm) PTFE and (<36 μm) PVC fragments	River water	H_2O_2
[72]	(10–100 μm) PP microspheres	City's coastal marine water	H_2O_2 30 %, 5 h, 70 °C
[40]	(1, 10, 40, 150 and 400 nm) PS microspheres, 12 μm PVDF, 12.5 μm PVDC, 23 μm ECTFE, 3 μm PTFE, 23 μm PFA, 20 μm PP, 20 μm PE, 30 μm PET, PVC ≤ 50 μm, PMMA ≤ 50 μm	Simulated water doped with PS microspheres (400 nm, 40 μm), tap water, lake water	H_2O_2 15 %, 15–18h
[49]	(10–45 μm) PE, (50 μm) PS, (50 μm) PP microspheres, Grinded and sieved (20–45 μm) PP fragments	Size-fractionated (5–45 μm) and density-extracted lake water	H_2O_2 30 % Fe^{2+} catalyse (20 mL 0.05 M $FeSO_4$), 75 °C
[79]	(1, 5, 10, and 20 μm) PS microspheres	Bottled water from artificially aged PET bottles	H_2O_2 3 %, 24 h, 50 °C

et al. introduced hyperspectral stimulated Raman scattering imaging as a promising advancement in Raman spectroscopy for NP analysis. They found that more that 90 % of the quantified MNPs measure between 100 nm and 1 μm [55]. It highlights again the need to improve small MNPs quantification, especially on the sub-micrometer range. To address this critical gap, this review focuses on a novel methodology combining fluorescence labelling with Nile Red (NR) and flow cytometry (FC), which has recently emerged as an efficient and automated approach for rapidly quantifying MNPs, especially NPs. This recently developed two-step method based on light scattering and fluorescence, allows the detection of particles whose sizes are on the order of the wavelength used, including those smaller than a micron. It allows automated quantification of MNPs ranging in size from 0.2 to 100 μm [35]. This promising method involves fluorescent labelling of MNPs with NR followed by optical identification and quantification using a FC [3]. Since its introduction in 2020, this method has been adopted and investigated by various researchers, each utilizing distinct protocols. This review aims to comprehensively describe this method summarize the current state of knowledge on its applications and limitations for MNP detection, and identify key areas where further research is needed to enhance its utility and reliability. By addressing these objectives, we hope to provide a clearer framework for standardizing and improving MNP quantification methodologies, particularly at the nanoscale, highlighting its promising prospects, limitations, and potential biases that could affect accurate qualitative analysis and measurement.

Literature search and data collection

An extensive literature search was conducted up to November 2024 across scientific databases, including Web of Science and Google Scholar. The search strategy employed a combination of keywords—'microplastics,' 'Nile Red,' 'dye,' 'staining,' and 'flow cytometry'—utilizing Boolean operators (AND/OR). From the retrieved articles, those specifically focusing on the fluorescent staining of microplastics with NR for quantification via FC were selected. A total of nine articles met these criteria, with >50 % published in China and 2/3 focusing on water samples (either potable or from environmental sources). These studies consistently used standard samples to calibrate their methodologies before analyzing actual samples. The operational conditions, MP standards employed, and flow cytometry parameters utilized are detailed in Tables 1, 2 and 3.

Flow cytometry analysis

FC is an analytical method that uses radiation-matter interactions to detect, identify, quantify, or sort particles in a liquid medium [1,76]. The schematic description of the FC is given in Fig. 1. The sample containing the particles is analysed in liquid form. A pump first aspirates a volume of the liquid sample. This volume is transported at a constant flow rate in front of a laser where particles are aligned (or focused) for analysis. The pressure difference between the sample and sheath fluid, creates a smooth flow where individual particles can sequentially pass in front of a laser for analysis [65]. The focusing step is essential and significantly impacts the quality of the analysis. Generally, this focusing is achieved by a sheath fluid (usually a phosphate-buffered saline solution). This liquid forms a concentric cylinder around the liquid capillary containing the sample, increasing the pressure around this capillary and thus reducing its diameter to align the particles along its axis. This focusing step ensures the particles pass one-by-one through the analysis zone, or flow cell. Other methods, such as acoustic focusing, which generates a vibratory frequency to force alignment, are

Table 2
Flow cytometers and their analysis parameters for the quantification of MNPs coupled with NR. NM: Not mentioned; /: no threshold applied on this parameter.

Reference	FC model	Fluidic parameters		Optics and fluorescence parameters			
		Analysed volume	Flow rate (µL/min)	Laser (nm)	Detector (nm)	Threshold	Voltage (mV)
[35]	Attune NxT Acoustic Focusing Cytometer Thermo Fisher Scientific	NM	25	638 (100 MW) 488 (50 MW)	695/40 FSC SSC	/ / 100	360 140 280
[71]	Bio-rad ZE5 Cell Analyzer, Hercules	100 µL	10	488/10	FSC SSC 583/30 509/24	0.01 % / / /	140 280 425 615
[57]	Attune NxT Acoustic Focusing Cytometer Thermo Fisher Scientific	NM	12.5	401 561	SSC 585/16	NM	NM
[70]	Bio-rad ZE5 Cell Analyzer, Hercules	100 µL	10	488/10	FSC 583/30 SSC	0.01 % / /	140 425 280
[7]	BD Accuri C6 flow cytometer, BD Biosciences	100 µL	35	488	FSC SSC 535/10	NM	NM
[72]	Bio-rad ZE5 Cell Analyzer, Hercules	100 µL	10	488/10	FSC 583/30 SSC	0.01 % / /	140 425 280
[40]	Guava easyCyte, Luminex, BD Biosciences	NM	NM	488	FSC SSC 583/26 695/5 525/30	NM	140 280 430 610 100
[49]	BD Influx Mariner, Becton Dickinson / Cytopeia	“1-drop into 9 mL glass vials”	NM	488	531/40 FSC	100mV 100mV	NM
[79]	CytoFLEX, Beckman Coulter, Brea	30µL	30	488	FSC 695/30		Gain 248 Gain 544

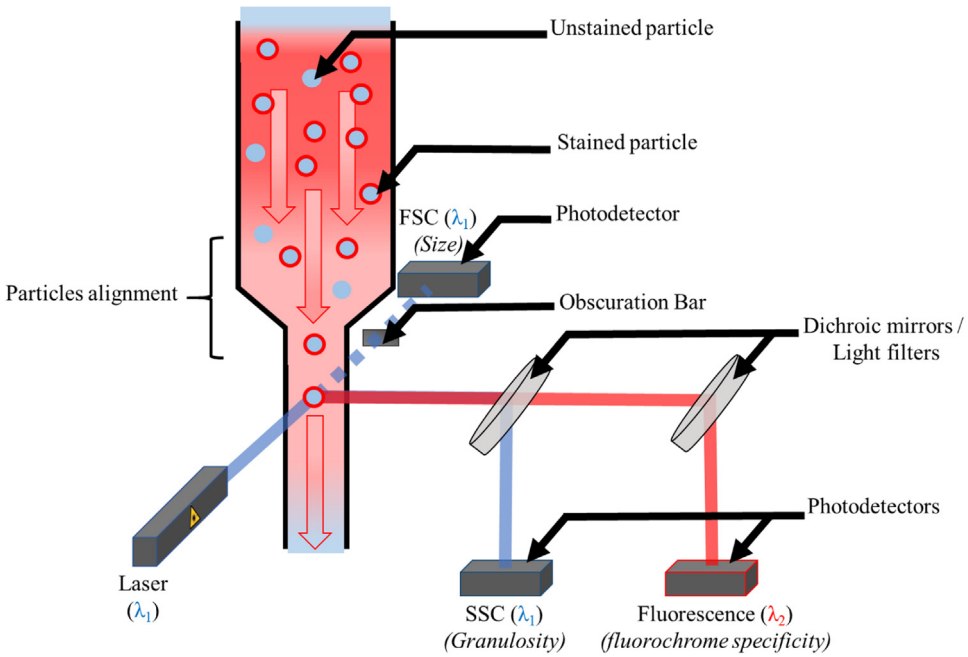

Fig. 1. Schematic representation of the flow cytometer with the alignment of particles, the diffusion parameters (FSC and SSC) and the fluorescence parameter measurements.

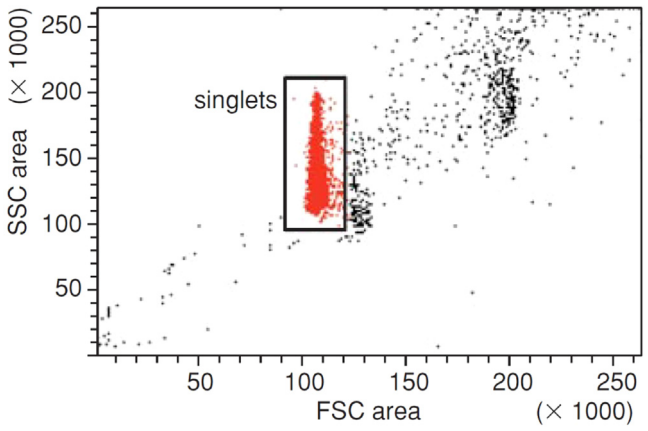

Fig. 2. Example of singlet gating based on FSC area signal, illustrated on a Dot-Plot of SSC peak area versus FSC peak area obtained using calibration beads, adapted from [32].

also available [25]. Once aligned in the counting chamber, the particles are each detected by one or more lasers arranged in series. The light signals resulting from the interactions between the particle and the laser will be detected, and their intensities will enable differentiation of the particles based on these interactions. Thanks to the control of the analysed volume, the concentrations of the different particle populations present in the sample are determined. This however requires an integrated volumetric measurement, an air bubble and particle free sheath fluid and an intact sample lines [13]. It should be noted that this injection step is rapid and can be automated, enabling the successive analysis of multiple samples and facilitating studies across a wide range of samples.

Optical analysis involves irradiating each particle individually with one or more monochromatic wavelengths, generally produced by lasers, to measure the corresponding signal intensity across various light passbands, coupled to photomultiplier tubes (PMTs).

The optical analysis is primarily based on the elastic scattering of light by the particles. As a particle passes in front of the laser, the light is scattered in all directions according to Mie scattering principles. Detectors positioned either along the same axis or at approximately 90° to the laser beam measure forward scatter (FSC) and side scatter (SSC), respectively [1,65]. An obscuration bar is placed between the counting zone and the FSC detector. This allows the detector to measure intensity only when light is scattered by a particle. FSC and SSC parameters indicate cell size and granularity, respectively, enabling the use of scattered intensities for qualitative purposes [1]. The intensity given by the detector is proportional to the scattering cross section, which depends on the refractive index of the medium and the refractive index of the particle, meaning only relative sizes and granulometries for particles made of the same material can be estimated [20]. By calculating the angular distribution of scattered light as a function of the particles size and refractive index, Mie theory can still relate the scattered power measured by the FSC detector to particle sizes. It has been shown that there was a good linearity between PS microspheres sizes and FSC signal [20,74].

Introducing additional measurement parameters allows a more precise differentiation of different types of particles. This can be achieved through fluorescence, where lasers with specific wavelengths excite dyes, and the emitted light during de-excitation is detected within the desired emission interval. In fluorescence analysis, the dyes on the sample emit light at specific wavelengths, enabling further discrimination between materials. Notably, flow cytometers can be equipped with multiple lasers placed in series along the sample path, allowing for the simultaneous analysis of particles labelled with different dyes. Fluorescence photons are first filtered by band pass filters and then detected by detectors placed at 90° to the laser optical path. The measured wavelength is not a monochromatic wavelength but rather the range of wavelengths filtered by the bandpass. It is expressed as *λ / width of the filtered range*. For example, for em. 583/26 nm the sensor is sensitive to wavelengths ranging from 570 nm to 596 nm.

Each PMT, with its corresponding passband, is designed to measure a specific parameter, allowing to analyse the signal intensity for each parameter of every particle. This enables the construction of histograms for each parameter to show the number of events measured at each intensity. To represent a more complex outcome for the entire sample, graphs displaying two parameters are created. These are called “Dot-Plots” or “density Plots” where each point represents a measured event and the intensities for these parameters are shown in arbitrary units [1,76]. It should be noted that the measured events are expected to correspond to particles, but they may also include background noise. The use of arbitrary units, depending on FC optical configuration and sensitivity, makes data interpretation and comparison between different FC complicated [20]. Thresholding is applied to remove low-intensity signals detected by PMTs, which is useful for eliminating signals from electronic noise [4,65].

Clusters of points, corresponding specific populations, can be observed on Dot-Plots [73]. Counting zones, or gates, can be drawn around those clusters to count particles within that region, enabling the quantification of each population separately. However, signal values, typically derived from the height or area of the pulse resulting from Mie scattering or fluorescence, can vary. Those variations are influenced by parameters such as alignment with the laser, particle morphology, size, refractive index, the range of the dichroic mirror, and detector sensitivity [32,65]. The boundaries of these counting zones can be drawn by the operator or generated by algorithms, introducing potential bias due to human or computer error, or subjective interpret [13,65]. Therefore, distinct zones must have a significant gap between them to ensure coherent quantification [13]. Fig. 2 illustrates the application of a gate to differentiate

particles passing individually in front of the detector from those passing in pairs, based on the intensity measured by integrating the pulse signal of FSC [32]. In this case, only events within the rectangular gate is counted as singlets while all other events, background noise or clusters, are excluded.

Nile red and flow cytometry

Definition and history of Nile red

Fluorescence is a powerful tool in analytical chemistry or biology, enabling specific compounds identification through fluorescence targeted labelling. When exited by a radiation, the dye used to stain the target will emit a radiation which wavelength differs from the excitation source. This property allows for precise detection and analysis of complex samples enhancing visibility and differentiation of otherwise indistinguishable components [41]. Labelling also improves the sensitivity of photosensitive analytical devices by increasing the intensity of emitted light, which enables the detection of smaller MPs [22].

NR adsorbs on MNPs through Van der Waals or dipole-dipole interactions [45]. It belongs to the benzophenoxazine family with a compact aromatic structure that provides high stability and intense fluorescence [34,46]. Its diethylamino group makes it suitable for labelling MPs due to their physicochemical affinities [3]. Historically, the benzophenoxazine family has first been used in biology to observe lipids inside cells [28], and it has been applied to polymers for the first time to estimate and to compare the polarity of various films [21]. It is only over the past decade, NR has increasingly been applied in MNPs analysis [64]. It has proven very useful for analysing MPs in various environmental matrices and food packaging [10,47,68,75,78], allowing for more precise microscopic observation of MPs, reducing false positives and increasing recovery rates [45,63].

The diethylamino group in NR can rotate relative to the rest of the molecule upon photon absorption [26]. These rotations, influenced by the polarity of surrounding molecules, typically the solvent, affect the molecule's dipole moment and internal electric field distribution [29], which alters optical properties. Consequently, NR's excitation and emission wavelengths depend on the medium's polarity, making NR a solvatochrome. Its excitation and emission wavelengths are 553 nm and 635 nm in methanol, respectively [23]. Its absorption and emission wavelengths range from 484 nm and 529 nm in n-heptane to 591 nm and 657 nm in water, respectively [28].

The NR staining process presents several challenges. Sample preparation and measurement involve variable parameters that must be adjusted to optimize result quality. It is crucial to prepare a concentrated NR stock solution by dissolving the powder in an appropriate solvent and storing it in the dark at low temperatures to preserve its fluorescent properties. The choice of solvent and NR concentration affects the dye's attachment to MPs, NR dissolution, fluorescence intensity, and absorption and emission bands [35]. Shruti et al. listed fluorescence intensities measured on common polymers and indicated that most major polymer families fluoresce under certain conditions [64].

Flow cytometry coupled with Nile red staining in the biological field

FC is a well-established method in the medical and biological fields as it allows for the analysis of cells and bacteria [1], where many dyes can be used to distinguish and quantify different populations [76]. Despite their small size, ranging from 0.2 µm to 50 µm for most of the bacterias and from 0.2 µm to few hundreds of micrometers for cells [6], FC enables quantitative analysis of different populations mixed in a single sample [1].

Greenspan et al. were the first to develop a NR application in FC to quantify lipid droplets formation induced by incubation of mouse macrophages [28]. With stock solutions at different concentrations in acetone, they investigated the ability of NR to allow differentiation lipid loaded cells from others by increasing their fluorescence intensity at 557.5/22.5 nm and at wavelengths above 610 nm. They observed an increase in fluorescence intensity at $\lambda > 610$ nm by increasing NR concentration from 0.1 µg/mL to 1 µg/mL. They considered that the dye in the medium could not interfere with lipid droplets fluorescence because of the quenching of its fluorescence in water. Within the same year, in order to better understand NR selectivity, they studied micro-emulsions of lipids and other lipophilic cells by fluorescence spectroscopy [27]. They noted a high fluorescence with neutral lipid-rich lipoproteins and produced strong fluorescence and weak fluorescence with hydrophilic proteins, concluding on a lipophilic specificity of the dye.

In 2003, a study on lipid quantification in algae employed solvatochromic properties of NR to quantify the proportion of neutral and polar lipids in cells [19]. The average yellow and red fluorescence intensities provided by flow cytometry with 488 nm excitation were used to determine the relative proportions of neutral and polar lipids, respectively. The method was later optimized for a wide range of samples. Incubation time and temperature, NR concentration [16,17], addition of co-solvent (dimethyl sulfoxide (DMSO) 40 %), pH adaptation (6.5) [58], fluorescence wavelengths optimisation have been studied for various applications [36].

Flow cytometry coupled with Nile red staining for quantification of microplastics and nanoplastics

Primarily, FC technology has been applied to MPs, without the use of NR [8,38,42,50,62]. This application has enabled the counting of particles ranging in size from 1 µm to 100 µm. Due to the highly variable sizes and morphologies of plastic particles, they cannot initially be easily differentiated from other potential particles in the sample. To address this, the method has been enhanced by the introduction of NR staining [35,57,71]. Only particles with NR molecules on their surface emit fluorescent radiation, allowing them to be discriminated from other particles. MNPs labeling can also enhance the fluorescent signal, enabling better differentiation from background noise and other unstained particles, particularly NPs, which exhibit weak diffusion signals due to their small size

[13,35,40]. This improvement facilitates clearer distinction and reduces the lowest measurable size by FC, which are key factors in MNPs analysis. This method has since been reused in several articles, with some modifications to the labelling protocol, analytical parameters, and data processing [7,40,49,70,72,79].

Advantages of the method

This technique based on Mie scattering enables the detection of particles with sizes near to the wavelength of the laser used. It offers accessible, fast and cost-effective routine quantification of a substantial amount of MNPs dispersed in liquid media. Indeed, it provides shorter analysis times and lower detection limits compared to traditional vibrational spectroscopy techniques, which detect MPs from 20 µm for FTIR spectroscopy to 1 µm for Raman spectroscopy [1,53], and can go under 1 µm for the few most cutting-edge methods [55]. Its ability to quantify NPs is one of the strengths of FC. It has been observed that the number of NPs is significantly higher than that of MPs [57,61,70,79] and the same trend applies to toxicity levels [18,31,43].

Conducting analysis in a dispersed liquid phase can eliminate the need for filtration steps in some cases. By assuming that the dispersion is homogeneous and that losses due to MNPs adhering to the walls are negligible, the preparation process is simplified and potential losses are avoided. Finally, the method allows for the analysis of samples with a flow rate ranging from 12 µL/min to 1 mL/min. This enables systematic quantification of particles present in the sample within a short timeframe. Thousands of particles are thus analysed within minutes, enabling robust statistical analysis. It is important to adjust the flow rate according to the concentration of the sample to prevent an excessive number of particles from passing through the detector simultaneously, which could affect accuracy.

Sample compositions

Analytical method is usually first developed on artificial medias, which we will refer to here as calibration samples in order to set the right analysis parameters. Artificial medias can be described in two categories: synthetic microspheres provided from different suppliers, or artificial fragments, generated by scratching [35] or grinding [7,49] of larger plastic items, or directly purchased as fragments [40,71]. Fragments can also be sorted by size with a filtration or a sieving step [7,35,49,71]. Many polymer types, listed in Table 1 like polypropylene (PP), polyethylene (PE), polystyrene (PS), polyethylene terephthalate (PET), polyvinyl chloride (PVC), high-density polyethylene (HDPE), low-density polyethylene (LDPE) , polymethyl methacrylate (PMMA), polylactic Acid (PLA), polytetrafluoroethylene (PTFE), polyvinylidene fluoride (PVDF), polyvinylidene chloride (PVDC), ethylene chlorotrifluoroethylene (ECTFE) and perfluoroalkoxy alkane (PFA) have been analysed as known sample with FC. The developed protocol is then generally applied to real samples including aquatic samples [7,49,71,72], drinking water [70,79], human peripheral blood [57], or samples simulating real samples, with pre-filtered aquatic samples doped with spherical MNPs [40].

Experimental media pre-treatment

In order to quantify MNPs only, environmental samples can be pre-treated depending on the type of media. First, particles bigger than FC tubes could lead to FC clogging, involving analysis failure and a potential damage to the device. Then, the lipophilic properties of NR allows it to stain other non-plastic hydrophobic particles and their presence could result to false positives [64]. Organic treatments operated on real samples are summarized in Table 1. Only Minor et al. removed inorganic contents in their lake water samples by density separation using a NaCl solution with a density of 1.15 g/mL [49]. A multi filtration stage can also be applied to analyse MNPs based on the particle size range [40,49]. It enables to provide results within specific size ranges.

Analytical protocol

After the possible sample processing, the analysis begins with the incubation step. Here, the sample is labelled with a small volume of stock solution containing dissolved NR and stored, or incubated, in the dark. The stock solution of NR is made in a solvent with lower polarity than water such as DMSO [35,40], acetone [49], methanol [7], or ethanol [70–72] at a concentration of 1 mg/mL. After the incubation, where NR adsorbs on the MNPs, an aliquot of the sample is introduced into the flow cytometer by aspiration at a controlled flow rate. The scattered light (FSC and SSC) is mainly studied at 488 nm, excepted with Salvia *et al.* who used a 401 nm laser [57]. NR fluorescence can be studied with different excitation (ex.) and emission (em.) wavelengths.

Currently, there is no consensus on the specific device parameters to use for quantifying MNPs by FC. These parameters, listed in Table 2, might need to differ depending on the equipment, particles analysed, impurities, or the fluid used. These parameters include excitation wavelengths (laser used) and emission wavelengths (band pass filters used). The Dot-Plots or histograms generated are used to spot the fluorescence intensity of NR on the selected channel and depend on the applied parameters and the capabilities of the device. A method development should initially be performed in order to identify the right parameters and the specific gate framing the events corresponding to MNPs.

The selected bandpass containing the wavelength emission, which is longer than the excitation wavelength, is variable depending on the article. The voltages applied to the detectors can also vary between studies. Although these voltages influence the relative intensity measured on each channel, they affect the relative position of the plots and thus of the different populations on the Dot-Plots. It is essential to adjust the detector sensitivity to distinguish measured events from background noise while avoiding event saturation and their intensity reaching the maximum measurable by the detector [65].

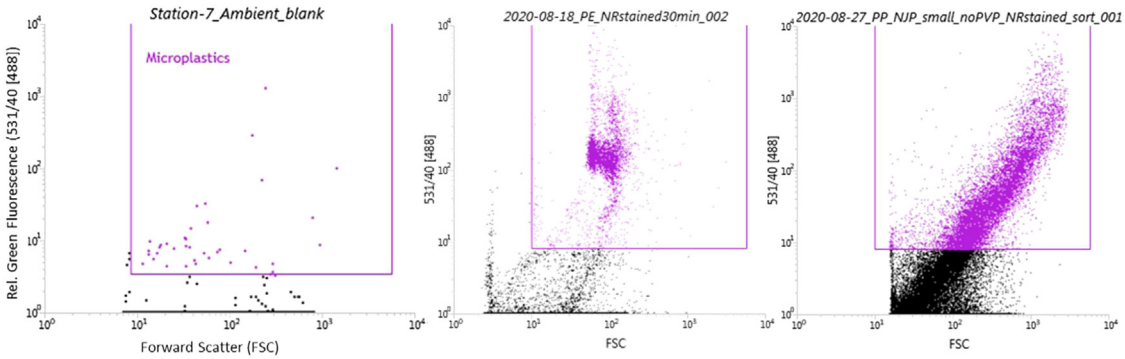

Fig. 3. Example of parameter and gating calibration with side scatter versus green fluorescence (531/40 nm) with blank (left), PE microspheres (middle) and ground PP samples (right), stained with NR at 10 µg/mL at room temperature for 30 mins. Blank and microspheres samples have been filtered between staining step and FC analysis, adapted from [49].

Table 3
Size and quantities of MNPs detected and quantified by FC coupled with NR. Some values have been calculated from raw data in order to normalize measured concentrations of samples. NM: not mentioned.

Reference	Size range	Fluorescent particles concentration range measured by FC (particle/mL) *(Raw values measured in cytometry tubes, before any conversion is done)*		
		Stained blank samples	Calibration samples	Real samples
[35]	0.2–100 µm	NM	10^5 – 10^7	/
[71]	1–50 µm	NM	$3.3.10^2$ – $5.68.10^4$	$3.74.10^5$
[57]	0.2–1 µm	10^4	NM	$3.2.10^5$ – $6.5.10^6$
[70]	1–50 µm	1200	2380	863 – $8.94.10^3$
[7]	0.6–15 µm	$3.43.10^4$	$8.23.10^4$	$1.2.10^3$–$2.7.10^4$
[72]	1–50 µm	NM	NM	$1.16.10^4$–$3.88.10^5$
[40]	0.2–50 µm	10^3–10^4	10^4–10^7	$1.5.10^5$–3.10^5
[49]	3–45 µm	10^2	$3.78.10^2 \pm 41$	$6.24.10^5$–$1.79.10^6$
[79]	1–100 µm	31	NM	28–74

Authors use different solutions and instrument settings in order to spot the populations of interest. Usually, authors use blank samples consisting of a stained sample without MNPs to evaluate background or parasite signals on the different parameters. They then analyse calibration stained samples in order to determine which gate is the best to quantify the MNPs population.

The gate is drawn around the MNPs population. Then, the “real” sample, consisting of an experimental sampling of water is analysed using same parameters, and the number of MNPs it contains is obtained. The Fig. 3 shows the resulting Dot-Plots of an FC analysis of a method blank, a calibration sample containing PE microspheres (10–45µm) and a sample of ground PP. Tests are all stained using a NR concentration of 10 µg/mL, irradiated with a blue light excitation (488 nm) and detected with a 531/40 nm bandpass filter and the SSC parameter. Gating to quantify MPs is performed to the regions highlighted in purple on the Dot-Pots.

In this case, the two parameters voltages are set to make the sphere population stand out at median intensity values, high enough to stand out from the noise and low enough so that the signals do not saturate. The gate is then to quantify subsequent samples.

Other particles present in the medium or noise are thus excluded, and MPs can be identified and quantified. Indeed, in the absence of NR, MNPs and background noise-associated signals can overlap, preventing MNPs quantification [35].

Microspheres, due to their size monodispersity, are easily gated on Dot-Plots. However, two issues can still be noted on that case. First, some events appear within the gate in the pre-filtered blank sample (217 to 255 event/mL), indicating presence of false positives. Then, it comes to actual plastic fragments that resemble MPs found in environmental media, the presence of events with varying fluorescence and scattering signals results in signal dispersion that starts at the background noise level. There is thus a continuum of events ranging from signals with low to high fluorescence. As a result, distinguishing between events that correspond to noise or background and those from the MNPs is not straightforward. Gate boundaries, supposed to be placed in areas with low point density to minimize gating-related variations, are instead positioned where the concentration of events is not negligible, leading to significant bias in distinguishing the populations. This bias affects both the quantification of MPs and the exclusion of noise. Those issues will be discussed later.

Results

The Table 3 indicates the quantities of MNPs in blank, calibration and real samples. Some values are not given explicitly in the publications and have been determined by calculation. The different experimental procedures do not allow a simple comparison of

the results as they stand. There is no correlation between the quantity of MNPs measured and the size range studied. In tree of the six papers that provide concentrations measured in blank samples, the values obtained in the blanks are greater than those in the actual samples, or at least not negligible. This highlights that some measured events in real samples may not necessary be MNPs from the sample.

Method limitations

NR aggregation issue

Several researchers have observed that NR, due to its hydrophobic nature, forms aggregates in predominantly aqueous samples. Indeed, during the staining step, NR previously dissolved in a relatively low polar solvent is abruptly introduced into an aqueous solution, leading to a partial precipitation and aggregates formation within the sample. These aggregates exhibit similar fluorescence properties to labelled MNPs and can appear in the same regions of the Dot-Plots as MNPs, complicating the delineation of counting areas and quantification of MNPs. The boundaries of counting areas on Dot-Plots could be indeed within continuous point clouds rather than at their edges, raising questions about potential overlap between the two populations [35]. Interpretations regarding their fluorescence behaviour are variable and raise concerns about the presence of false positives in the gates used for MNP quantification.

Authors have worked on resolving this last issue by many means. This issue was fist mentioned by *Kaile* et al. who were the firsts to use NR coupled with FC to quantify a number of event [35]. Li et al. investigated the detection limit for MNPs (400 nm – 40 μm) stained with NR at various concentrations [40]. They quantified their calibration samples using two approaches: one that ignored the presence of NR aggregates and another considered them by subtracting their concentration in the counting zone of blank samples. They found that considering NR aggregates could result in an overestimation of about 20 %. Additionally, they concluded that, in the condition of their experiments, the presence of NR aggregates resulted in a limit of detection of 10^4 particle/mL.

MNPs size and shape dispersity

MNPs can be found in many medias, in a wide range of sizes and shapes. FC scattering parameters are sensitive of those properties. Analysis on real samples are thus much more complicated than a sample made only with monodisperse PS spheres. This complexity arises from the signal dispersion caused by these differences, which leads to signals that blend with background noise.

Microplastics and nanoplastics size approximation

Calibration charts have been generated with monodisperse microspheres with various sizes in to link FSC or SSC signals to particle sizes [7,72,79]. Authors used additivated PS beads with various sizes and established a calibration line [7] or curve [72]. This chart can then be used to estimate the size of experimental particles with unknown dimensions. Microspheres have also been used to determine a detection size limit, where the particle signal merges with the background signal [35,79], or to set a size limit, by applying a threshold just below the lowest scattering value measured from a the corresponding microspheres population. As described before, there is a good linearity between PS microspheres sizes and FSC delivered intensity. However, it should be noted that this intensity also depends on the refractive index of the detected particle, which implies that the calibration chart is not applicable to all types of materials. At ambient temperature, pure PS refractive index value is around 1.59, when PP and PE refractive indexes are 1.50 and 1.51, respectively [5]. Moreover, light scattering differs between spherical particles and irregularly shaped particles, leading to variations in light intensity [14]. A study with more realistic plastic fragments with varying and mastered sizes, natures and granularities should be conducted to assess the validity of this calibration.

Gate establishment

Due to the continuum caused by the NR aggregates presence and the size polydipersity of the fragments, deciding where to draw the gates to split dots population is questionable. Moreover, the gating process is performed manually by the operator, which can introduce bias into the results, especially when populations overlap. Consequently, quantification of MNPs might be arbitrary. It is reasonable to assume that for some heterogeneous samples the two parts of the split point cloud contain both stained MNPs and NR aggregates.

Nile red relatively low microplastics and nanoplastics specificity

First, a method involving NR labelling is thus limited by the same constraints as its epifluorescence counterpart: it can be biased by the presence of nonpolar organic matter leading to false positives [64] and it does not enable the identification of the polymeric nature. Tse et al. investigated this issue by voluntarily introducing organic carbon in blank samples [71,72]. They observed a significant increasing of false positives while raising the amount of organic carbon. They also showed that H_2O_2 treatment could reduce this false-positive signal by 47.7–94.2 %.

Surface polarity of the microplastics and nanoplastics

NR is an hydrophobic dye and an increasing surface polarity of the MNPs could lead to a loss of compatibility and prevent the quantification [52]. Polymers with polar chemical functions are indeed less able to be quantified by microscopy coupled with NR staining [64]. Furthermore, weathering can alter surface chemistry of polymers and reduce the ability of NR to bond to MNPs [15], making the analysis process harder for natural samples.

Instrument clogging

FC is constrained by the internal diameter of its tubing, which can become clogged when particles are too large. The equipment is typically equipped with mechanisms to reverse the clogging by reversing the flow to dislodge the stuck particles. However, such incidents can disrupt the analysis and potentially cause irreversible damage to the system, which must be avoided.

Cross-Contamination issues and cleaning process

Due to the adhesive nature of MP particles, authors have adapted the rinsing protocol between different samples to maintain the cleanliness of fluidic lines and avoid cross-contamination. No rinsing solution has yet been unanimously established, but the issue has been raised on several occasions. The authors can use pure water [57,70–72], or water combined with surfactants or non-polar solvents to improve compatibility with MNPs and thus MNP release. Kaile et al. used a Milli-Q water solution with 10 % DMSO [35]. They still observed cross-contamination phenomena despite cleaning. Li et al. used a solution between 10 and 30 % DMSO for their rinsing [40]. Salvia et al. use an alkaline solution of Helmanex III (Attune NxT Flow Cell Cleaning Solution, Cat# A43635) composed mainly of surfactants as well as Contrad 70 (Beckman Coulter, Ref# 81,911), a concentrated liquid detergent that is phosphate-free, chlorine-free, and biodegradable [57]. It is worth noting that MNPs blocked between the FC input and the counting cell are not quantified and constitute a loss during quantification. Instruments equipped with pump system can often reverse the direction of the fluidics in order to remove a plug from the tubing [13].

Issue of microplastics and nanoplastics heterogeneity in dispersion and minimal required concentration

The volume taken from the tube has to be representative of the entire sample. The method therefore involves a uniform dispersion of MNPs in the tube. First, MNPs should neither agglomerate nor sediment. Moreover, they should not adhere to the tube or position themselves at the air/water interface. Tse et al. used a surfactant (Tween 20) at 0.1 % w/v to reduce the surface tension of particles and thus improve particle dispersion [71,72]. FC also requires to acquire a significant number of events for statistical analysis [13]. Bianco et al. showed that the number of MNPs should be included between 10^4 and 10^6 particle/mL for this reason [7]. Environmental samples could therefore be pre-concentrated. Tse et al. claim that pre-concentration not only removes soluble organic carbon, but also dissolved salts in natural waters, which increase the surface tension of the medium and hinder the proper dispersion of MNPs [71]. Samples with a low concentration of MNPs would be difficult to analyse considering that this concentration has to be significantly higher than the signal from blank for quantification.

Method development and issues solving

Main issues and corresponding optimisations

The main issue, highlighted since the method application to MNPs in 2020 [35], which has been investigated is NR aggregation. Authors addressed this challenge measuring the absorbance of the solution by UV–Vis spectroscopy at 549 nm. The goal was to minimize the presence of crystals while maintaining effective staining of plastic particles. The tests were based on two criteria: the absorbance, which should be maximal, and the stability of this absorbance at the time of labelling and 10 mins after, corresponding to the state after incubation [35]. Tse et al. based the efficiency of their method on the recovery rate value based on a quantity of MNPs measured by fluorescence microscopy [71]. Li et al. based their criteria on the distinction of the two fluorescent populations on the Dot-Plots [40]. It requires minimizing the population of aggregates on the Dot-Plots as much as possible. Although the number of events measured in this population is not provided, the Dot-Plots are displayed, and distinctions are made based on visual inspection.

Sample composition

Polarity modification

In order to improve NR solubility, lowering the polarity of the medium can be a valuable approach. Kaile et al. examined the addition of co-solvents such as DMSO, ethanol, and methanol in proportions ranging from 10 % to 75 % [35]. The optimal co-solvent was found to be DMSO at 55 %, although 35 % ethanol or 40 % methanol also showed good results. DMSO has been chosen due to its previous use with their FC. Tse et al. adapted the protocol developed by Kaile et al. by eliminating the use of a co-solvent but introducing 0.1 % w/v of Tween 20, a surfactant, to promote the dispersion of MNPs by reducing their surface tension in water. They used a labelled blank to perform a correction excluding the aggregate population observed in the blanks for low-intensity FSC signals. This method allowed them to distinguish most calibration beads from the aggregate population, except for the smaller beads,

Table 4
Staining conditions of the samples tested by FC coupled with NR. NM: not mentioned. RT: room temperature.

Reference	Country	NR Stock solution solvent	[NR] working solution (mg/mL)	Sample solution compo-sition	[NR] incub-ation (µg/mL)	Incub-ation time	Incubation temper-ature
[35]	Ireland, Norway	DMSO (99.9 %), ethanol (95 %), and methan-ol	1	DMSO 10 %	10	10, 30, and 60 min	22 °C
[71]	China	95 % ethanol	1	Tween 20; 0.1 %(w/v)	10	10 min	RT
[57]	Spain	NM	1	H_2O	0.2	15 min	RT
[70]	China	95 % ethanol	1	Tween 20; 0.1 %(w/v)	10	10 min	RT
[7]	Finland, Italy, France	methanol	1	DMSO 10 %	10	30 min	NM
[72]	China	95 % ethanol	1	Tween 20; 0.1 %(w/v)	10	10 min	RT
[40]	China	DMSO	0.2	DMSO 10–30 %	15	10 min	RT
[49]	USA	acetone >99.5 %	1	H_2O	10	30 – 60 min	RT
[79]	China	NM	NM	H_2O	NM	NM	NM

setting the detectable minimum size at 1 µm. This approach was adopted in their subsequent articles [70–72]. Minor et al., for the same reasons, used another surfactant, polyvinylpyrrolidone at 3 %, only for their calibration samples [49]. In 2023, Li et al. studied the use of DMSO at different proportions and the addition of 0.1 % w/v Polysorbate 20 (Tween 20). They determined that a DMSO concentration between 20 % and 30 % was optimal for NR dissolution, improving the separation of aggregates and MPs, and that the use of Tween 20, at these proportions, did not allow for good dissolution of aggregates [40]. They also tested labelling efficiency using PS microspheres at 10 µm in 15 % DMSO for four stock solution solvents (DMSO, ethanol, acetone, and acetonitrile). DMSO was selected because it produced the least background noise. No significant effect of pH, between 3 and 10 with the addition of variable volumes of 0.1 M HCl or NaOH, was observed for MNPs suspended in Milli-Q water with 10 % DMSO and 0.1 % Tween 20 [35].

To date, all studies exploring the use of a co-solvent to reduce sample polarity to enhance NR solubility and thus reduce NR aggregates have confirmed the effectiveness of this approach. Among the tested options, DMSO has been identified as the most suitable solvent, with optimal concentrations ranging from 10 % to 30 %. Increasing the proportion of organic solvent is nevertheless limited by the fragility of sample lines with respect to often aggressive solvents. A device dedicated to MNP analysis using this method could be designed, with materials inert to organic solvents. The sheath fluid usually consists of a phosphate buffered saline solution with high polarity due to the ions presence [13]. Changing this fluid could be a good way to reduce aggregates presence.

Nile red concentration

Kaile et al. also tested 10 % DMSO solutions for different concentrations of NR in UV–Vis (1, 10, 100, and 1000 µg/mL) [35]. They determined that the optimal concentration was 10 µg/mL, as the absorbance difference before and after incubation was minimal, with almost zero absorbance. Li et al. studied the effects of NR concentration (0, 2.5, 5, 7.5, 10, 15, and 20 µg/mL) on PP, PET, and PS by comparing the number of particles observed in the counting area with the theoretical number of added MPs, providing insights into NR aggregate concentrations. In order to effectively stain PET, which is more polar than PP or PE, the NR concentration was set at 15–20 µg/mL, successfully labeling over 90 % of PET, PE, and PP. Other NR parameters, such as the solvent used to prepare the NR stock solution, incubation time and temperature can be adjusted. No study has yet determined the right parameters with FC, which might depend from one sample to another, based on factors like polymer type, particles concentration, impurities. Parameters applied to the NR stock solution and incubation parameters are shown in Table 4.

NR concentration effect on aggregates issue has also been investigated by microscopy in aqueous media [9]. They investigated drinking water samples and aqueous samples spiked with a known amount of 100 nm and 2 µm PS nanospheres. Using a 1.2 W laser diode at 520 nm, with emission filtered by a long-pass filter blocking light below 561 nm and a stock solution of NR in methanol at 1 mg/mL, the study investigated the number and size of NR aggregates as a function of NR concentration. First, with blank samples without MNPs, it was shown that decreasing NR concentration reduces the number and size of NR aggregates. They observed that a maximum concentration of 30 nM should be applied to avoid larger, extremely bright and often needle-like structures crystal formation in blank samples, typical of a recrystallization of NR after dissolution. With PS beads, they found that concentration under 15 nM are too low to stain correctly the MNPs, resulting in an underestimation, and should be avoided. They also observed aggregates of NR with concentrations under 60 nM, but their quantity (<50 particle/mL) was negligible compared to the concentration of beads (20,130 particle/mL). In comparison, NR concentrations used in flow cytometry studies range from 0.2 µg/mL ($n = 1$) to 15 µg/mL ($n = 1$), with most studies using 10 µg/mL ($n = 6$). These concentrations correspond to 628 nM, 47,100 nM, and 31,400 nM, respectively, which are all significantly higher than the maximum concentration determined in microscopy. Investigations on NR concentration by FC have indeed conclude an optimal concentration above 10 µg/mL, where effectiveness of staining and presence of aggregates have a good balance [35,40]. Li et al. stated that concentrations under this value lead to a superposition between unstained ([NR] = 0 µg/mL) and stained particles on the Dot-Plots [40]. It should however be noted that Chatterjee et al. did not investigate the use of co-solvent such as DMSO in their study.

Sample pre-concentration

To improve the sensitivity and accuracy of the method, a pre-concentration step can be performed through filtration, followed by transferring the sample to a smaller volume [40,71,72,79]. This requires a filter that prevents MNPs from adhering to its surface. For the samples used by both Tse et al. and Li et al., the filter exhibiting the better desorption efficiency has been identified as the Mixed Cellulose Ester (MCE) type, achieving a transfer rate of 94.9 ± 7.1 % [71] or 82.56 % [40]. This step also provides a reduction of organic matter with size below the pore size, lowering the background of the FC analysis. It is important to note that the detection limit of this pre-concentration step is constrained by the pore size of the filter.

A high concentration of MNPs makes it possible to ignore the presence of non-plastic aggregates or particles in the gates, since their number could become negligible compared with the concentration of MNPs. This is why a pre-concentration step may be necessary to estimate MNP concentrations accurately, even in the presence of NR aggregates [7,71,79]. As noted by Li et al., a NR background concentration of 10^3–10^4particle/mL in blank samples involve a minimum MNPs concentration of 10^4particle/mL in order to overcome false positive interferences [40]. Some samples, though, are so diluted that analysing them via FC would require a concentration increase by a factor of 10^7 to 10^8. This highlights two potential areas for improvement in future investigations. First, as previously mentioned, the reduction of NR aggregates remains an issue that requires further exploration. Second, there is a need for rapid and effective methods to concentrate MNPs in diluted samples.

Sample pre-filtration

In order to prevent FC from clogging, some authors add a pre-filtration step to their samples prior to the staining step, with metal or stainless steel membranes (45–50 μm), prior the staining step [40,49,71,72]. This step sets the maximum size measured by the analysis.

Preparation techniques

Kaile et al. attempted to stain MNPs on paper filters and then transfer them to solution for FC analysis. However, they found that the MNPs remained stuck to the filter and that this additional manipulation could introduce contamination [35]. To minimize NR aggregates in the aqueous sample, a pre-filtration step can be introduced after staining and before analysis, ensuring aggregates are removed in the filtrate while stained MPs remain on the filter cake. Minor et al. opted for pre-filtration on a 10 μm nylon filter to remove NR aggregates before FC analysis. The cake was then suspended in deionized water and filtered through a 100 μm nylon mesh to remove aggregates that might block the 200 μm nozzle tip during FC analysis. This procedure was performed on blanks and plastic standards for development, but the first 10 μm filtration step was not used for field samples to avoid potential losses during resuspension. This can explain the continuum of dots observed in the real sample, in contrast to the absence of events in the blank sample shown in Fig. 3. This demonstrates that a pre-filtration step can effectively reduce NR aggregates, enabling more accurate MNP quantification. Note that this procedure increases the lower size limit to 10 μm [49], and may result in losses of MNPs due to their adherence to the filter [35,40]. Transfer methods, including vortexing, ultrasonication, and homogenization, were studied with pre-filtration using an MCE filter. Ultrasonication proved to be the most effective, achieving transfer rates of 90.31 % and generating the fewest MCE particles that could interfere with MNPs quantification [40].

Filtration and sonication of the staining solution were also tested before the staining step to remove any pre-existing aggregates. The filtration process helps suppress aggregates that are smaller than the filter pore size, while sonication breaks weak bonds between NR molecules, effectively disrupting and dissolving NR aggregates. Li et al. used a stock NR solution at 1 mg/mL in DMSO filtered through a 50 μm stainless steel mesh after a 10-minute ultrasonic treatment, then through a 0.22 μm filter to remove precipitates and aggregates before each labelling. Three filters were tested (glass fiber, MCE, and nylon), with the glass fiber filter chosen for its efficiency and because it did not introduce impurities interfering with MNP quantification [40]. Their results illustrate the advantage of filtering and sonicate the labelling solution before labelling samples, with a removal efficiency of 58 % with glass fiber filter and a reduction of aggregates. They also optimized temperature (25 °C and 60 °C) and incubation time (10min, 30 min, 1 h, and 2 h) on PS microspheres, showing that PS exhibited a strong signal at both temperatures as well as all incubation times studied.

Preparation processes similar to filtration or sonication have proved effective in removing aggregates [35,40,70]. However, this step should be conducted after MNPs staining to eliminate small aggregates, thereby reducing the number of false positives while maintaining a sufficient staining efficiency. Filtration using an MCE membrane is recommended due to its low particle adsorption on the surface. With sonication, it is possible that even after effective dissolution, aggregates may reappear soon after. Indeed, although solubilized in the stock solution, NR aggregates are observed after sonication, suggesting that dissolution in a predominantly aqueous medium leads to this precipitation [40]. To prevent NR aggregation, it is essential to keep the NR concentration below its solubility limit during sample analysis. If this condition is not met, NR will inevitably precipitate, regardless of the precautions taken in previous steps.

Flow cytometer configuration and data analysis

An overlap in the Dot-Plots between NR aggregates and stained MNPs increase the risk of false-positives measurement and may be a significant source of bias for quantification.

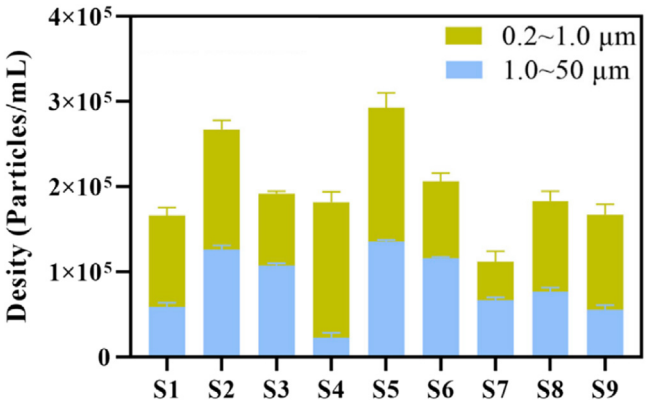

Fig. 4. particle concentration of MP (blue) and NP (green) in 9 simulated water samples measured by FC: 3 ultrapure water samples (S1–S3), 3 tap water samples (S4–S6), and 3 lake water samples (S7–S9). Adapted from [40] under the Creative Commons Attribution License (CC BY) [40].

Flow cytometer configuration and gating strategy

As shown before, some variations can arise from Mie scattering or fluorescence influenced by factors such as laser alignment, dichroic mirror range, detector sensitivity, particle morphology, size, and refractive index. Therefore, parameters might be adjusted for each new study. The discrimination process being performed manually by the operator can introduce a bias in the results.

Kaile et al. adapted their gating strategy using the parameter ex. 638 nm em. 695/40 nm to differentiate NR aggregates, attributed to high-intensity signals, from labelled plastic particles, attributed to low-intensity signals [35]. These intervals vary depending on the type of MP quantified. They concluded that the distinction between these two populations was achievable for PS, PE, PET, and PC, while PVC, PP, PA, LDPE, and HDPE were partially obscured by aggregates on the Dot-Plots [35]. Bianco et al., on the other hand, observed by spectrofluorometry that NR aggregates in an aqueous NR solution at 10 μg/mL did not have fluorescence properties [7]. They therefore considered that all events measured with significant fluorescence intensity for 488 nm ex. 530/40 nm em. corresponded to MNPs. Minor et al. considered that NR aggregates number was only significant in “red fluorescent” Dot-Plots and used “green fluorescence” at 531/40 nm to quantify stained MNPs [49]. Li et al. identified the best counting areas on SSC vs. yellow and yellow vs. red [40]. They found, according to the quantity of fluorescent particles detected through 23 NR-stained blanks and 26 NR-stained PS microspheres, that yellow fluorescence is more intense in stained MPs than in NR aggregates, unlike red fluorescence, where aggregates and MNPs have the same fluorescence intensity. They plotted the gate on the Dot-Plot of SSC versus 583/26 nm emission because of its low quantity of fluorescent particles in the blanks and because the diversity of results obtained with this gate is lower than with other.

Blank subtraction

To deal with background noise registered in blank samples within the counting regions, some authors have calculated the concentration of stained MNPs by subtracting the concentration of background noise measured from the concentration of fluorescent particles measured in MNPs samples [35,40,49,70,72,79]. However, this correction implies three prerequisites to be correctly used: first, the quantity of event measured into the blank samples gates should be relatively stable so that the results do not vary too much. It is essential to minimize pre-analytical variations during the collection, processing, and storage stages [13]. Finally, the number of fluorescent events in the blank sample must be negligible compared to the number of events in the MNPs sample.

Example of quantification with improvements

Following numerous protocol enhancements aimed at maximizing the ratio between stained MNPs and NR aggregates—by minimizing aggregates and using concentrated samples—Li et al. successfully quantified a significant amount of MNPs in their samples [40]. Their study demonstrated quantifications performed on nine pre-filtered water samples spiked with PS microspheres. As shown Fig. 4, after a multistage filtration process and subtraction of the blank value, ranging from 10^3 to 10^4 particles/mL, they were able to accurately quantify microplastics (blue) and nanoplastics (green). This result, deemed acceptable in relation to their blank value and exceeding it by an order of magnitude, highlights the effectiveness of the previously discussed improvements.

Discussion and recommendations

FC coupled with NR staining is one of the most promising methods on MP quantification for its many advantages. Compared to traditional methods, FC coupled with NR enables faster quantification of MNPs, reducing both time and labor requirements, while achieving improved size detection limits by identifying smaller particles. Its ability to automatically process numerous samples facilitates multiple repetitions to address variations from media heterogeneity and allows for more efficient analysis of samples from diverse locations. This can lead to a clearer and more accessible understanding of the widespread presence of MNPs in the

Table 5
Alternative dyes tested for MPs staining and MPs they were tested on.

Author / Year	Dyes	MNPs	Staining conditions
[52]	Acridine Orange, Basic Blue 24, Crystal Violet, Lactophenol Blue, Neutral Red, Safranin-T, Trypan Blue	LDPE, HDPE, PP, PS, expanded Polystyrene (EPS), cellulose acetate (CA), PVC, nylon, weathered HDPE, PE, PE fibers, PP, EPS and CA.	T°amb., 10 µg/mL, 30 min
[44]	Fluorescein isophosphate, Safranine T	Plastic powders: PE, PVC, PS, PET,	25 °C, 50 °C, 75 °C, 100 °C, 10 µg/mL, 10 min, 20 min, 30 min
[45]	Oil Red EGN, Eosin B, Rose Bengal, Hostasol Yellow 3G	Scratched macroplastics : PE, PP, PS, PET, PVC, nylon	T°amb., 10 µg/mL, 60 min
[11]	Coumarin 6, coumarin 7, coumarin 30	3–5 mm pellets: LDPE, HDPE, PP, PS, PC, PMMA, PA, PVC. Cutted PET film (5 × 5 × 0.3 mm), EPS 3–5 mm spheres	T°amb., 0.5, 1.0, 5.0, and 10 µg/mL, 30 min, 60 min, 180 min

environment. However, several significant limitations have been identified that could hinder the achievement of analytically reliable results.

Recent studies have provided interesting leads for solving the problems inherent in the method. However, there are still issues to address, with two major ones that should be solved first. The first one involves NR aggregates, whose population is still overlapped on the population of marked disperse MPs, and the dispersity of MNP shapes, resulting in a signal continuum that starts in the background noise, thereby hindering accurate gating and quantification. The main objectives here are to increase the quantity of labeled MNPs in relation to the fluorescent signals attributed to other components and to permit a confident gate drawing with well-defined dot clouds separated from background even for irregularly shaped fragments. It should be noted that, despite the numerous improvements made by Li et al. to reduce NR background concentration, they still measured a concentration of NR aggregates/background noise ranging between 10^3 and 10^4particle/mL in the counting zone with their blank samples [40]. This highlights the need of further development but also to be cautious when interpreting the results. With the results provided by the authors who contributed to the development of the method, several major improvements put forward by the authors, but also suggested avenues can be mentioned for future work on the subject, which will be resumed here.

Suggested improvement

Nile red substitution with other dyes

Other dye, with higher solubility in aqueous media could be considered to avoid aggregates formation. Comparative studies between NR and other hydrophobic dyes have been conducted with fluorescent microscopy. The Table 5 shows the four studies that compared NR with other candidates, with the tested dyes and the MNPs they were tested on. Maes et al. and Lv et al. both concluded that NR was the most suitable for this application because of its better compatibility and fluorescence intensity compared to other tested fluorochromes [44,45]. However, Lv et al. concluded that raising the temperature at 50 °C could allow Fluorescein isophosphate and Safranine T to stain most of the tested MNPs when Fluorescein isophosphate still needs a covalent bond creation with the surface of the MNPs. It was shown by Prata et al. that among tested dyes, including Safranin T, NR was the only one able to stain all the nine tested plastics [52]. Chouchene et al. successfully quantified MPs stained with Eosin B with a cross validation by FTIR with Attenuated Total Reflectance [12].

Sturm et al. modified NR by substituting ethyl groups with longer chains (Ethylhexyl, n-Hexyl) to improve hydrophobicity and added a polar 2-propionic acid group to stain polar MPs like PVC [67]. They tested these derivatives on various polymers and natural particles, finding the effects highly dependent on the dye-polymer combination. The 2-propionic acid derivative showed good fluorescence for most polymers, and its polar nature may enhance water solubility and compatibility with FC. Cheng et al. investigated Coumarin dyes in non-polar solvents, finding Coumarin 6 effective, though its performance in polar conditions has yet to be evaluated. [11]. It is worth noting that solubility criterium has not been considered because of the analytical technique, which is done on a filter and thus is not concerned by a solubilisation of the used dyes. Only Tong et al. investigated the fluorescence stability of the tested fluorochrome, Rhodamine B, and found it to be suitable for application in aqueous media [69].

Adding complementary fluorochromes could also be an effective way to further subdivide heterogeneous populations. By adding an additional fluorescent signal to a specific component of the population and make, it becomes distinguishable using other measurement parameters (ex./em.). However, this approach has so far only been applied to NR stained MP in order to differentiate them from biological components [48,66].

It should however be noted that a better fluorochrome solubility in water might induce a lower specificity with MNPs. Nevertheless, fluorochromes with lower specificity can still be beneficial for enhancing signal strength or when working with controlled samples.

Filtration after staining

Stained sample could be filtered before analysis to remove NR aggregates, with a resuspension of the filter content in a filtered solution [49]. While this does raise the detection limit for quantifying MNPs based on size and potentially involves particle loss, it can also potentially break the signal continuum, allowing for more accurate gating by filtering out smaller microplastics and aggregates. The MCE membrane filter is actually the most suitable filter to achieve this step [40,71].

Flow cytometer adaptation

It has been shown that organic solvents enhance NR solubilisation, reducing number of NR aggregates. However, such products present several challenges. First, FC tubing are designed for aqueous medias and the materials used in their construction are not suitable for organic solvents which can react with plastics and potentially damage device components. Finally, the sheath fluid used to focus particles prior to detection is composed of a saline and highly polar solution, which may need to be replaced with a significantly different solvent. This approach requires adapting the FC system and making substantial modifications, particularly in developing a focusing step that accommodates significantly different fluids.

Some FC are equipped with an integrated camera allowing an imaging coupling with diffusion and fluorescence analysis [30]. This first allows a verification of a correct gating but it can also be used with deep learning to identify aggregates which possess needle like structures and can be identified by the right algorithms [9,30]. Their use could enhance distinction between MNPs and aggregates and thus greatly enhance this method.

Complementary protocol validation

A complementary study on NR precipitation in various medias adapted to FC, could provide new information or solutions to the method limitations. This method has already been complemented by gas chromatography coupled with pyrolysis [49], but a technique providing concentration in terms of the number of events could serve as a good way to validate the method regarding aggregates issue. A cross-validation with recognized spectroscopic techniques as micro Raman or micro FTIR could allow a better assessment of the method robustness.

Investigating the precipitation mechanisms and their kinetics may lead to a more precise understanding of this phenomenon. Furthermore, investing the combination of DMSO and a surfactant could result in a solution allowing aggregates reducing and MNPs dispersion within the sample tube.

Finally, validation of the size calibration of the method, conducted using micro-beads designed for analytical devices calibration [7,72], should be supplemented with real MNPs fragments of various natures, shapes and granularities. Using filters with various pore sizes, a sample containing MNPs of different sizes could be separated into solutions with a narrower particle size distribution. This would allow for a more precise investigation of the separation between noise and MNPs in the Dot-Plot.

Data processing complexity increasing

To answer populations overlapping problems in Dot-Plots, or with the use of several colorants, it is possible to study more than two parameters in order to better separate populations [40]. Manually drawing boundaries on several two-parameters plot and combining them can enhance population separation, but this makes data processing more difficult and time-consuming [13]. For example, Sgier et al. managed to differentiate many biofilm populations without using any dye, only using scattering and fluorescence signals coupled "visual stochastic network embedding" data analysis [62].

Several different parameters have already been used to isolate populations of MNPs. Due to this reason, the numerous variations in MNPs and parameters used, or the gating biases, it is currently impossible to establish a standardized protocol for data acquisition and treatment.

Results expression

In order to facilitate comparisons between the different results and a better understanding of the improvements made to the method, the results should be given exhaustively for the control samples and the real samples. Because of the problem of NR precipitation, the numbers of events measured in the zones attributed to the aggregates, but also in the blanks, should be systematically provided, with corresponding standard deviations. This allows verification that the number of aggregates in the contact zones is negligible compared with the number of labelled MNPs and confirms that the results are analytically valid.

Regarding the size ranges of the analysed particles, caution is needed when directly comparing irregularly shaped MNPs from real samples to calibration PS spheres due to differences in shape and refractive index. Cross-validation using an imaging technique or an integrated camera would be advisable.

Raised improvement

List of major improvement

- Filter all FC fluids (e.g., sheath fluid, cleaning solutions), sample solutions (water, NR solvent) or NR stock solutions using non-plastic filters to remove contaminants or NR aggregates.
- Analyse only high-concentration MNP samples ($>10^4$ particle/mL) to minimize signal / noise ratio; apply robust pre-concentration steps for low-concentration samples.
- Samples should contain at least 10 % DMSO to limit NR precipitation; additional methods to lower sample polarity while preserving NR staining are needed. Use surfactants like Tween 20 to improve MNP dispersion, though not for NR dissolution.
- Establish minimal NR concentrations necessary for effective MNP distinction while minimizing aggregation (e.g., 10 μg/mL with 10-minute incubation).
- Ensure thorough washing between samples, regularly run blanks to prevent cross-contamination, and report results with blank concentration data for accuracy. Subtract blank events from sample counts when significant, considering their standard deviation.

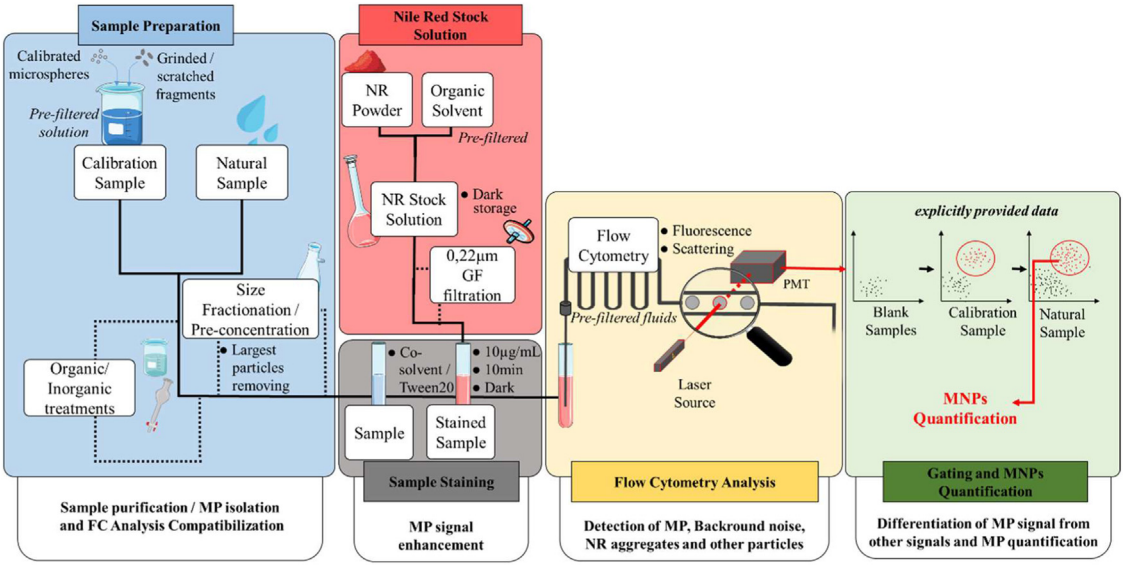

Fig. 5. Schematic representation of the full quantification process of MNPs by FC.

Overview diagram

The Fig. 5 summarises the key stages in the protocol for quantifying MNPs by flow cytometry, from sample preparation to interpretation of the results.

Conclusion

This review provides an exhaustive description of the several steps involved in the analysis of MNPs by FC, with a particular focus on the miscellaneous issues inherent in this method. Its advantages over spectroscopic methods like speed, automation, and detection limits have been compared to the locks that remain to be unlocked to be analytically reliable. To quantify MNPs correctly, the ratio of stained MNPs to background noise must indeed be maximized. Pre-concentrating MNPs or performing additional steps to minimize NR aggregates background noise in the sample are the most straightforward and effective approaches to address this issue. Enhancements such as filtering or sonicating the stained sample prior to analysis are among the most promising approaches. Moreover, adjusting the sample composition—such as by adding components to reduce NR aggregates or pre-concentrating the sample to render NR aggregates negligible—could further enhance reliability. Additionally, NR aggregation variability across studies highlights the importance of increasing NR solubility within samples and including blank sample tests in publications to validate analytical parameters and ensure data accuracy, paving the way for future improvements in MNP quantification. Due to the multiplicity of tested samples and applied parameters, a standardized protocol for data acquisition remains elusive. Therefore, developing a standardized protocol for robust data acquisition is crucial, including a collaboration between MNP experts and flow cytometry manufacturers. This would aid the simultaneous development of the method alongside the equipment, significantly enhancing the studies on plastic pollution by providing more accurate data on MNPs in various ecosystems.

Ethics statements

None.

Credit author statement

Lucas Ainé: Conceptualization, Writing - original draft, Writing – review – editing, Methodology, Investigation. **Justine Jacquin:** Investigation, Supervision. **Colette Breysse:** Investigaation, Supervision. **Catherine Colin:** Investigation, Supersion, Project administration. **Jean-Michel Andanson:** Conceptualization, Writing – review – editing, Methodology. **Florence Delor-Jestin:** Conceptualization, Writing – review – editing, Methodology, Project administration.

Declaration of competing interest

The authors declare that they have no known competing financial interests or personal relationships that could have appeared to influence the work reported in this paper.

Acknowledgments

This research was funded by CT-IPC (Industrial Technical Center for Plastics and Composites) and the ANRT (Association Nationale de la Recherche et de la Technologie: CIFRE Grant N 2021/1410).

References

[1] A. Adan, G. Alizada, Y. Kiraz, Y. Baran, A. Nalbant, Flow cytometry: basic principles and applications, Crit. Rev. Biotechnol. 37 (2017) 163–176, doi:10.3109/07388551.2015.1128876.
[2] L.F. Amato-Lourenço, R. Carvalho-Oliveira, G.R. Júnior, L. Dos Santos Galvão, R.A. Ando, T. Mauad, Presence of airborne microplastics in human lung tissue, J. Hazard. Mater. 416 (2021) 126124, doi:10.1016/j.jhazmat.2021.126124.
[3] A.L. Andrady, Microplastics in the marine environment, Mar. Pollut. Bull. 62 (2011) 1596–1605, doi:10.1016/j.marpolbul.2011.05.030.
[4] G.J.A. Arkesteijn, E. Lozano-Andrés, S.F.W.M. Libregts, M.H.M. Wauben, Improved flow cytometric light scatter detection of submicron-sized particles by reduction of optical background signals, Cytometry. a 97 (2020) 610–619, doi:10.1002/cyto.a.24036.
[5] A.A. Askadskiĭ, Computational Materials Science of Polymers (2003).
[6] L.L. Barton, D.E. Northup, Microbial Ecology (2011).
[7] A. Bianco, L. Carena, N. Peitsaro, F. Sordello, D. Vione, M. Passananti, Rapid detection of nanoplastics and small microplastics by Nile-Red staining and flow cytometry, Environ. Chem. Lett. 21 (2023) 647–653, doi:10.1007/s10311-022-01545-3.
[8] A. Bringer, H. Thomas, G. Prunier, E. Dubillot, N. Bossut, C. Churlaud, C. Clérandeau, F. Le Bihanic, J. Cachot, High density polyethylene (HDPE) microplastics impair development and swimming activity of Pacific oyster D-larvae, crassostrea gigas, depending on particle size, Environ. Pollut. 260 (2020) 113978, doi:10.1016/j.envpol.2020.113978.
[9] S. Chatterjee, E. Krolis, R. Molenaar, M.M.A.E. Claessens, C. Blum, Nile red staining for nanoplastic quantification: overcoming the challenge of false positive counts due to fluorescent aggregates, Environ. Chall. 13 (2023) 100744, doi:10.1016/j.envc.2023.100744.
[10] S. Chen, Y. Li, C. Mawhorter, S. Legoski, Quantification of microplastics by count, size and morphology in beverage containers using Nile Red and ImageJ, J. Water Health 19 (2021) 79–88, doi:10.2166/wh.2020.171.
[11] Y. Cheng, J. Zhang, H. Nakano, N. Ueyama, H. Arakawa, Coumarin 6 staining method to detect microplastics, Mar. Pollut. Bull. 193 (2023) 115167, doi:10.1016/j.marpolbul.2023.115167.
[12] K. Chouchene, J.P. Da Costa, A. Wali, A.V. Girão, O. Hentati, A.C. Duarte, T. Rocha-Santos, M. Ksibi, Microplastic pollution in the sediments of Sidi mansour harbor in southeast tunisia, Mar. Pollut. Bull. 146 (2019) 92–99, doi:10.1016/j.marpolbul.2019.06.004.
[13] A. Cossarizza, H. Chang, A. Radbruch, A. Acs, D. Adam, S. Adam-Klages, W.W. Agace, N. Aghaeepour, M. Akdis, M. Allez, L.N. Almeida, G. Alvisi, G. Anderson, I. Andrä, F. Annunziato, A. Anselmo, P. Bacher, C.T. Baldari, S. Bari, V. Barnaba, J. Barros-Martins, L. Battistini, W. Bauer, S. Baumgart, N. Baumgarth, D. Baumjohann, B. Baying, M. Bebawy, B. Becher, W. Beisker, V. Benes, R. Beyaert, A. Blanco, D.A. Boardman, C. Bogdan, J.G. Borger, G. Borsellino, P.E. Boulais, J.A. Bradford, D. Brenner, R.R. Brinkman, A.E.S. Brooks, D.H. Busch, M. Büscher, T.P. Bushnell, F. Calzetti, G. Cameron, I. Cammarata, X. Cao, S.L. Cardell, S. Casola, M.A. Cassatella, A. Cavani, A. Celada, L. Chatenoud, P.K. Chattopadhyay, S. Chow, E. Christakou, L. Čičin-Šain, M. Clerici, F.S. Colombo, L. Cook, A. Cooke, A.M. Cooper, A.J. Corbett, A. Cosma, L. Cosmi, P.G. Coulie, A. Cumano, L. Cvetkovic, V.D. Dang, C. Dang-Heine, M.S. Davey, D. Davies, S. De Biasi, G. Del Zotto, G.V. Dela Cruz, M. Delacher, S. Della Bella, P. Dellabona, G. Deniz, M. Dessing, J.P. Di Santo, A. Diefenbach, F. Dieli, A. Dolf, T. Dörner, R.J. Dress, D. Dudziak, M. Dustin, C. Dutertre, F. Ebner, S.B.G. Eckle, M. Edinger, P. Eede, G.R.A. Ehrhardt, M. Eich, P. Engel, B. Engelhardt, A. Erdei, C. Esser, B. Everts, M. Evrard, C.S. Falk, T.A. Fehniger, M. Felipo-Benavent, H. Ferry, M. Feuerer, A. Filby, K Filkor, S. Fillatreau, M. Follo, I. Förster, J. Foster, G.A. Foulds, B. Frehse, P.S. Frenette, S. Frischbutter, W. Fritzsche, D.W. Galbraith, A. Gangaev, N. Garbi, B. Gaudilliere, R.T. Gazzinelli, J. Geginat, W. Gerner, N.A. Gherardin, K. Ghoreschi, L. Gibellini, F. Ginhoux, K. Goda, D.I. Godfrey, C. Goettlinger, J.M. González-Navajas, C.S. Goodyear, A. Gori, J.L. Grogan, D. Grummitt, A. Grützkau, C. Haftmann, J. Hahn, H. Hammad, G. Hämmerling, L. Hansmann, G. Hansson, C.M. Harpur, S. Hartmann, A. Hauser, A.E. Hauser, D.L. Haviland, D. Hedley, D.C. Hernández, G. Herrera, M. Herrmann, C. Hess, T. Höfer, P. Hoffmann, K. Hogquist, T. Holland, T. Höllt, R. Holmdahl, P. Hombrink, J.P. Houston, B.F. Hoyer, B. Huang, F. Huang, J.E. Huber, J. Huehn, M. Hundemer, C.A. Hunter, W.Y.K. Hwang, A. Iannone, F. Ingelfinger, S.M. Ivison, H. Jäck, P.K. Jani, B. Jávega, S. Jonjic, T. Kaiser, T. Kalina, T. Kamradt, S.H.E. Kaufmann, B. Keller, S.L.C. Ketelaars, A. Khalilnezhad, S. Khan, J. Kisielow, P. Klenerman, J. Knopf, H. Koay, K. Kobow, J.K. Kolls, W.T. Kong, M. Kopf, T. Korn, K. Kriegsmann, H. Kristyanto, T. Kroneis, A. Krueger, J. Kühne, C. Kukat, D. Kunkel, H. Kunze-Schumacher, T. Kurosaki, C. Kurts, P. Kvistborg, I. Kwok, J. Landry, O. Lantz, P. Lanuti, F. LaRosa, A. Lehuen, S. LeibundGut-Landmann, M.D. Leipold, L.Y.T. Leung, M.K. Levings, A.C. Lino, F. Liotta, V. Litwin, Y. Liu, H. Ljunggren, M. Lohoff, G. Lombardi, L. Lopez, M. López-Botet, A.E. Lovett-Racke, E. Lubberts, H. Luche, B. Ludewig, E. Lugli, S. Lunemann, H.T. Maecker, L. Maggi, O. Maguire, F. Mair, K.H. Mair, A. Mantovani, R.A. Manz, A.J. Marshall, A. Martínez-Romero, G. Martrus, I. Marventano, W. Maslinski, G. Matarese, A.V. Mattioli, C. Maueröder, A. Mazzoni, J. McCluskey, M. McGrath, H.M. McGuire, I.B. McInnes, H.E. Mei, F. Melchers, S. Melzer, D. Mielenz, S.D. Miller, K.H.G. Mills, H. Minderman, J. Mjösberg, J. Moore, B. Moran, L. Moretta, T.R. Mosmann, S. Müller, G. Multhoff, L.E. Muñoz, C. Münz, T. Nakayama, M. Nasi, K. Neumann, L.G. Ng, A. Niedobitek, S. Nourshargh, G. Núñez, J. O'Connor, A. Ochel, A. Oja, D. Ordonez, A. Orfao, E. Orlowski-Oliver, W. Ouyang, A. Oxenius, R. Palankar, I. Panse, K. Pattanapanyasat, M. Paulsen, D. Pavlinic, L. Penter, P. Peterson, C. Peth, J. Petriz, F. Piancone, W.F. Pickl, S. Piconese, M. Pinti, A.G. Pockley, M.J. Podolska, Z. Poon, K. Pracht, I. Prinz, C.E.M. Pucillo, S.A. Quataert, L. Quatrini, K.M. Quinn, H. Radbruch, T.R.D.J. Radstake, S. Rahmig, H. Rahn, B. Rajwa, G. Ravichandran, Y. Raz, J.A. Rebhahn, D. Recktenwald, D. Reimer, C. Reis E Sousa, E.B.M. Remmerswaal, L Richter, L.G. Rico, A. Riddell, A.M. Rieger, J.P. Robinson, C. Romagnani, A. Rubartelli, J. Ruland, A. Saalmüller, Y. Saeys, T. Saito, S. Sakaguchi, F. Sala-de-Oyanguren, Y. Samstag, S. Sanderson, I. Sandrock, A. Santoni, R.B. Sanz, M. Saresella, C. Sautes-Fridman, B. Sawitzki, L. Schadt, A. Scheffold, H.U. Scherer, M. Schiemann, F.A. Schildberg, E. Schimisky, A. Schlitzer, J. Schlosser, S. Schmid, S. Schmitt, K. Schober, D. Schraivogel, W. Schuh, T. Schüler, R. Schulte, A.R. Schulz, S.R. Schulz, C. Scottá, D. Scott-Algara, D.P. Sester, T.V. Shankey, B. Silva-Santos, A.K. Simon, K.M. Sitnik, S. Sozzani, D.E. Speiser, J. Spidlen, A. Stahlberg, A.M. Stall, N. Stanley, R. Stark, C. Stehle, T. Steinmetz, H. Stockinger, Y. Takahama, K. Takeda, L. Tan, A. Tárnok, G. Tiegs, G. Toldi, J. Tornack, E. Traggiai, M. Trebak, T.I.M. Tree, J. Trotter, J. Trowsdale, M. Tsoumakidou, H. Ulrich, S. Urbanczyk, W. Van De Veen, M. Van Den Broek, E. Van Der Pol, S. Van Gassen, G. Van Isterdael, R.A.W. Van Lier, M. Veldhoen, S. Vento-Asturias, P. Vieira, D. Voehringer, H. Volk, A. Von Borstel, K. Von Volkmann, A. Waisman, R.V. Walker, P.K. Wallace, S.A. Wang, X.M. Wang, M.D. Ward, K.A. Ward-Hartstonge, K. Warnatz, G. Warnes, S. Warth, C. Waskow, J.V. Watson, C. Watzl, L. Wegener, T. Weisenburger, A. Wiedemann, J. Wienands, A. Wilharm, R.J. Wilkinson, G. Willimsky, J.B. Wing, R. Winkelmann, T.H. Winkler, O.F. Wirz, A. Wong, P. Wurst, J.H.M. Yang, J. Yang, M. Yazdanbakhsh, L. Yu, A. Yue, H. Zhang, Y. Zhao, S.M. Ziegler, C. Zielinski, J. Zimmermann, A. Zychlinsky, Guidelines for the use of flow cytometry and cell sorting in immunological studies (second edition), Eur. J. Immunol. 49 (2019) 1457–1973, doi:10.1002/eji.201970107.
[14] Craig F. Bohren, Donald R. Huffman, Absorption and scattering by an arbitrary particle, Absorption and Scattering of Light by Small Particles (1998) 57–81, doi:10.1002/9783527618156.ch3.
[15] J.P. Da Costa, A.R. Nunes, P.S.M. Santos, A.V. Girão, A.C. Duarte, T. Rocha-Santos, Degradation of polyethylene microplastics in seawater: insights into the environmental degradation of polymers, J. Environ. Sci. Health Part A 53 (2018) 866–875, doi:10.1080/10934529.2018.1455381.
[16] T.L. Da Silva, A. Reis, R. Medeiros, A.C. Oliveira, L. Gouveia, Oil production towards biofuel from autotrophic microalgae semicontinuous cultivations monitorized by flow cytometry, Appl. Biochem. Biotechnol. 159 (2009) 568–578, doi:10.1007/s12010-008-8443-5.
[17] T.L. Da Silva, C.A. Santos, A. Reis, Multi-parameter flow cytometry as a tool to monitor heterotrophic microalgal batch fermentations for oil production towards biodiesel, Biotechnol. Bioprocess Eng. 14 (2009) 330–337, doi:10.1007/s12257-008-0228-8.
[18] E. Danopoulos, M. Twiddy, R. West, J.M. Rotchell, A rapid review and meta-regression analyses of the toxicological impacts of microplastic exposure in human cells, J. Hazard. Mater. 427 (2022) 127861, doi:10.1016/j.jhazmat.2021.127861.
[19] A. De La Jara, H. Mendoza, A. Martel, C. Molina, L. Nordström, V. De La Rosa, R. Díaz, J. Appl. Phycol. 15 (2003) 433–438, doi:10.1023/A:1026007902078.
[20] L. de Rond, F.A.W. Coumans, R. Nieuwland, T.G. van Leeuwen, E. van der Pol, Deriving extracellular vesicle size from scatter intensities measured by flow cytometry, Curr. Protoc. Cytom. 86 (2018) e43, doi:10.1002/cpcy.43.

[21] A.K. Dutta, K. Kamada, K. Ohta, Spectroscopic studies of nile red in organic solvents and polymers, J. Photochem. Photobiol. Chem. 93 (1996) 57–64, doi:10.1016/1010-6030(95)04140-0.
[22] G. Erni-Cassola, M.I. Gibson, R.C. Thompson, J.A. Christie-Oleza, Lost, but found with Nile red: a novel method for detecting and quantifying small microplastics (1 mm to 20 μm) in environmental samples, Environ. Sci. Technol. 51 (2017) 13641–13648, doi:10.1021/acs.est.7b04512.
[23] T.K. Fam, A.S. Klymchenko, M. Collot, Recent advances in fluorescent probes for lipid droplets, Mater. (Basel) 11 (2018) 1768, doi:10.3390/ma11091768.
[24] S.B. Fournier, J.N. D'Errico, D.S. Adler, S. Kollontzi, M.J. Goedken, L. Fabris, E.J. Yurkow, P.A. Stapleton, Nanopolystyrene translocation and fetal deposition after acute lung exposure during late-stage pregnancy, Part. Fibre Toxicol. 17 (2020) 55, doi:10.1186/s12989-020-00385-9.
[25] G. Goddard, J.C. Martin, S.W. Graves, G. Kaduchak, Ultrasonic Particle-Concentration For Sheathless Focusing of Particles For Analysis in a Flow Cytometer (2006).
[26] C.M. Golini, B.W. Williams, J.B. Foresman, Further solvatochromic, thermochromic, and theoretical studies on Nile Red, J. Fluoresc. 8 (1998) 10.
[27] P. Greenspan, S.D. Fowler, Spectrofluorometric studies of the lipid probe, nile red, J. Lipid. Res. 26 (1985) 781–789, doi:10.1016/S0022-2275(20)34307-8.
[28] P. Greenspan, E.P. Mayer, S.D. Fowler, Nile red: a selective fluorescent stain for intracellular lipid droplets, J. Cell Biol. 100 (1985) 965–973, doi:10.1083/jcb.100.3.965.
[29] C.A. Guido, B. Mennucci, D. Jacquemin, C. Adamo, Planar vs. twisted intramolecular charge transfer mechanism in Nile Red: new hints from theory, Phys. Chem. Chem. Phys. 12 (2010) 8016, doi:10.1039/b927489h.
[30] A. Gupta, P.J. Harrison, H. Wieslander, N. Pielawski, K. Kartasalo, G. Partel, L. Solorzano, A. Suveer, A.H. Klemm, O. Spjuth, I.-M. Sintorn, C. Wählby, Deep Learning in image cytometry: a review, Cytometry. a 95 (2019) 366–380, doi:10.1002/cyto.a.23701.
[31] R.C. Hale, M.E. Seeley, M.J. La Guardia, L. Mai, E.Y. Zeng, A global perspective on microplastics, J. Geophys. Res. Oceans 125 (2020) e2018JC014719, doi:10.1029/2018JC014719.
[32] R.A. Hoffman, Pulse width for particle sizing, Curr. Protoc. Cytom. 50 (2009), doi:10.1002/0471142956.cy0123s50.
[33] J.R. Jambeck, R. Geyer, C. Wilcox, T.R. Siegler, M. Perryman, A. Andrady, R. Narayan, K.L. Law, Plastic waste inputs from land into the ocean, Science (1979) 347 (2015) 768–771, doi:10.1126/science.1260352.
[34] J. Jose, K. Burgess, Benzophenoxazine-based fluorescent dyes for labeling biomolecules, Tetrahedron. 62 (2006) 11021–11037, doi:10.1016/j.tet.2006.08.056.
[35] N. Kaile, M. Lindivat, J. Elio, G. Thuestad, Q.G. Crowley, I.A. Hoell, Preliminary results from detection of microplastics in liquid samples using flow cytometry, Front. Mar. Sci. 7 (2020) 552688, doi:10.3389/fmars.2020.552688.
[36] T. Katayama, M. Kishi, K. Takahashi, K. Furuya, M.E.A. Wahid, H. Khatoon, N.A. Kasan, Isolation of lipid-rich marine microalgae by flow cytometric screening with Nile Red staining, Aquac. Int. 27 (2019) 509–518, doi:10.1007/s10499-019-00344-y.
[37] A.A. Koelmans, P.E. Redondo-Hasselerharm, N.H.M. Nor, V.N. De Ruijter, S.M. Mintenig, M. Kooi, Risk assessment of microplastic particles, Nat. Rev. Mater. 7 (2022) 138–152, doi:10.1038/s41578-021-00411-y.
[38] F. Le Bihanic, C. Clérandeau, B. Cormier, J.-C. Crebassa, S.H. Keiter, R. Beiras, B. Morin, M.-L. Bégout, X. Cousin, J. Cachot, Organic contaminants sorbed to microplastics affect marine medaka fish early life stages development, Mar. Pollut. Bull. 154 (2020) 111059, doi:10.1016/j.marpolbul.2020.111059.
[39] J. Lee, K.-J. Chae, A systematic protocol of microplastics analysis from their identification to quantification in water environment: a comprehensive review, J. Hazard. Mater. 403 (2021) 124049, doi:10.1016/j.jhazmat.2020.124049.
[40] J. Li, F. Huang, G. Zhang, Z. Zhang, X. Zhang, Separation and flow cytometry analysis of microplastics and nanoplastics, Front. Chem. 11 (2023) 1201734, doi:10.3389/fchem.2023.1201734.
[41] J.W. Lichtman, J.-A. Conchello, Fluorescence microscopy, Nat. Methods 2 (2005) 910–919, doi:10.1038/nmeth817.
[42] M. Long, I. Paul-Pont, H. Hégaret, B. Moriceau, C. Lambert, A. Huvet, P. Soudant, Interactions between polystyrene microplastics and marine phytoplankton lead to species-specific hetero-aggregation, Environ. Pollut. 228 (2017) 454–463, doi:10.1016/j.envpol.2017.05.047.
[43] Y. Luo, C.T. Gibson, C. Chuah, Y. Tang, R. Naidu, C. Fang, Raman imaging for the identification of Teflon microplastics and nanoplastics released from non-stick cookware, Sci. Total Environ. 851 (2022) 158293, doi:10.1016/j.scitotenv.2022.158293.
[44] L. Lv, J. Qu, Z. Yu, D. Chen, C. Zhou, P. Hong, S. Sun, C. Li, A simple method for detecting and quantifying microplastics utilizing fluorescent dyes - Safranine T, fluorescein isophosphate, Nile red based on thermal expansion and contraction property, Environ. Pollut. 255 (2019) 113283, doi:10.1016/j.envpol.2019.113283.
[45] T. Maes, R. Jessop, N. Wellner, K. Haupt, A.G. Mayes, A rapid-screening approach to detect and quantify microplastics based on fluorescent tagging with Nile Red, Sci. Rep. 7 (2017) 44501, doi:10.1038/srep44501.
[46] V. Martinez, M. Henary, Nile Red and Nile Blue: applications and syntheses of structural analogues, Chem. - Eur. J. 22 (2016) 13764–13782, doi:10.1002/chem.201601570.
[47] S.A. Mason, V.G. Welch, J. Neratko, Synthetic polymer contamination in bottled water, Front. Chem. 6 (2018) 407, doi:10.3389/fchem.2018.00407.
[48] S. Maxwell, H. Melinda K, F. Matthew, Counterstaining to separate Nile red-stained microplastic particles from terrestrial invertebrate biomass, Environ. Sci. Technol. 54 (2020) 5580–5588, doi:10.1021/acs.est.0c00711.
[49] E.C. Minor, U.D. Gomes, K.M. Schreiner, N.J. Poulton, E. Hendrickson, M.A. Maurer-Jones, Small microplastic particles in Lake Superior : a preliminary study coupling Nile red staining, flow cytometry and pyrolysis gas chromatography–mass spectrometry, Limnol. Oceanogr. Methods lom 3 (2023) 10582, doi:10.1002/lom3.10582.
[50] S. Morgana, B. Casentini, S. Amalfitano, Uncovering the release of micro/nanoplastics from disposable face masks at times of COVID-19, J. Hazard. Mater. 419 (2021) 126507, doi:10.1016/j.jhazmat.2021.126507.
[51] L. Peng, D. Fu, H. Qi, C.Q. Lan, H. Yu, C. Ge, Micro- and nano-plastics in marine environment: source, distribution and threats — A review, Sci. Total Environ. 698 (2020) 134254, doi:10.1016/j.scitotenv.2019.134254.
[52] J.C. Prata, V. Reis, J.T.V. Matos, J.P. da Costa, A.C. Duarte, T. Rocha-Santos, A new approach for routine quantification of microplastics using Nile Red and automated software (MP-VAT), Sci. Total Environ. 690 (2019) 1277–1283, doi:10.1016/j.scitotenv.2019.07.060.
[53] S. Primpke, S.H. Christiansen, W. Cowger, H. De Frond, A. Deshpande, M. Fischer, E.B. Holland, M. Meyns, B.A. O'Donnell, B.E. Ossmann, M. Pittroff, G. Sarau, B.M. Scholz-Böttcher, K.J. Wiggin, Critical assessment of analytical methods for the harmonized and cost-efficient analysis of microplastics, Appl. Spectrosc. 74 (2020) 1012–1047, doi:10.1177/0003702820921465.
[54] S. Primpke, C. Lorenz, R. Rascher-Friesenhausen, G. Gerdts, An automated approach for microplastics analysis using focal plane array (FPA) FTIR microscopy and image analysis, Anal. Methods 9 (2017) 1499–1511, doi:10.1039/C6AY02476A.
[55] N. Qian, X. Gao, X. Lang, H. Deng, T.M. Bratu, Q. Chen, P. Stapleton, B. Yan, W. Min, Rapid single-particle chemical imaging of nanoplastics by SRS microscopy, Proc. Natl. Acad. Sci. 121 (2024) e2300582121, doi:10.1073/pnas.2300582121.
[56] A. Ragusa, A. Svelato, C. Santacroce, P. Catalano, V. Notarstefano, O. Carnevali, F. Papa, M.C.A. Rongioletti, F. Baiocco, S. Draghi, E. D'Amore, D. Rinaldo, M. Matta, E. Giorgini, Plasticenta: first evidence of microplastics in human placenta, Environ. Int. 146 (2021) 106274, doi:10.1016/j.envint.2020.106274.
[57] R. Salvia, L.G. Rico, J. Petriz, Fast-screening Flow Cytometry Method For Detecting Nanoplastics in Human Peripheral Blood (preprint) (2022), doi:10.31219/osf.io/59e4v.
[58] G.G. Satpati, R. Pal, Rapid detection of neutral lipid in green microalgae by flow cytometry in combination with Nile red staining—An improved technique, Ann. Microbiol. 65 (2015) 937–949, doi:10.1007/s13213-014-0937-5.
[59] L. Schröter, N. Ventura, Nanoplastic toxicity: insights and challenges from experimental model systems, Small. 18 (2022) 2201680, doi:10.1002/smll.202201680.
[60] S. Schürch, M. Geiser, M.M. Lee, P. Gehr, Particles at the airway interfaces of the lung, Colloids Surf. B Biointerfaces 15 (1999) 339–353, doi:10.1016/S0927-7765(99)00099-5.
[61] D. Schymanski, C. Goldbeck, H.-U. Humpf, P. Fürst, Analysis of microplastics in water by micro-raman spectroscopy: release of plastic particles from different packaging into mineral water, Water. Res. 129 (2018) 154–162, doi:10.1016/j.watres.2017.11.011.
[62] L. Sgier, R. Freimann, A. Zupanic, A. Kroll, Flow cytometry combined with viSNE for the analysis of microbial biofilms and detection of microplastics, Nat. Commun. 7 (2016) 11587, doi:10.1038/ncomms11587.

[63] W.J. Shim, Y.K. Song, S.H. Hong, M. Jang, Identification and quantification of microplastics using Nile Red staining, Mar. Pollut. Bull. 113 (2016) 469–476, doi:10.1016/j.marpolbul.2016.10.049.
[64] V.C. Shruti, F. Pérez-Guevara, P.D. Roy, G. Kutralam-Muniasamy, Analyzing microplastics with Nile Red: emerging trends, challenges, and prospects, J. Hazard. Mater. 423 (2022) 127171, doi:10.1016/j.jhazmat.2021.127171.
[65] Staats, J., Divekar, A., McCoy, J.P., Maecker, H.T., 2019. Guidelines for gating flow cytometry data for immunological assays, in: McCoy, Jr, J.P. (Ed.), Immunophenotyping, Methods in Molecular Biology. Springer New York, New York, NY, pp. 81–104. https://doi.org/10.1007/978-1-4939-9650-6_5
[66] T. Stanton, M. Johnson, P. Nathanail, R.L. Gomes, T. Needham, A. Burson, Exploring the efficacy of Nile red in microplastic quantification: a costaining approach, Environ. Sci. Technol. Lett. 6 (2019) 606–611, doi:10.1021/acs.estlett.9b00499.
[67] M.T. Sturm, H. Horn, K. Schuhen, The potential of fluorescent dyes—Comparative study of Nile red and three derivatives for the detection of microplastics, Anal. Bioanal. Chem. 413 (2021) 1059–1071, doi:10.1007/s00216-020-03066-w.
[68] R. Sutton, S.A. Mason, S.K. Stanek, E. Willis-Norton, I.F. Wren, C. Box, Microplastic contamination in the San Francisco Bay, California, USA, Mar. Pollut. Bull. 109 (2016) 230–235, doi:10.1016/j.marpolbul.2016.05.077.
[69] H. Tong, Q. Jiang, X. Zhong, X. Hu, Rhodamine B dye staining for visualizing microplastics in laboratory-based studies, Environ. Sci. Pollut. Res. 28 (2021) 4209–4215, doi:10.1007/s11356-020-10801-4.
[70] Y.-T. Tse, S.M.-N. Chan, E.T.-P. Sze, Quantitative assessment of full size microplastics in bottled and tap water samples in Hong Kong, Int. J. Environ. Res. Public. Health 19 (2022) 13432, doi:10.3390/ijerph192013432.
[71] Y.-T. Tse, H.-S. Lo, S.M.-N. Chan, E.T.-P. Sze, Flow cytometry as a rapid alternative to quantify small microplastics in environmental water samples, Water. (Basel) 14 (2022) 1436, doi:10.3390/w14091436.
[72] Y.-T. Tse, H.-S. Lo, C.-W. Tsang, J. Han, J.K.-H. Fang, S.M.-N. Chan, E.T.-P. Sze, Quantitative analysis and risk assessment to full-size microplastics pollution in the coastal marine waters of Hong Kong, Sci. Total Environ. 879 (2023) 163006, doi:10.1016/j.scitotenv.2023.163006.
[73] A. Tzur, J.K. Moore, P. Jorgensen, H.M. Shapiro, M.W. Kirschner, Optimizing optical flow cytometry for cell volume-based sorting and analysis, PLoS. One 6 (2011) e16053, doi:10.1371/journal.pone.0016053.
[74] E. Van Der Pol, F.A.W. Coumans, A.E. Grootemaat, C. Gardiner, I.L. Sargent, P. Harrison, A. Sturk, T.G. Van Leeuwen, R. Nieuwland, Particle size distribution of exosomes and microvesicles determined by transmission electron microscopy, flow cytometry, nanoparticle tracking analysis, and resistive pulse sensing, J. Thromb. Haemost. 12 (2014) 1182–1192, doi:10.1111/jth.12602.
[75] K.J. Wiggin, E.B. Holland, Validation and application of cost and time effective methods for the detection of 3–500 μm sized microplastics in the urban marine and estuarine environments surrounding Long Beach, California, Mar. Pollut. Bull. 143 (2019) 152–162, doi:10.1016/j.marpolbul.2019.03.060.
[76] M.J. Wilkerson, Principles and applications of flow cytometry and cell sorting in Companion Animal medicine, Vet. Clin. North Am. Small Anim. Pract. 42 (2012) 53–71, doi:10.1016/j.cvsm.2011.09.012.
[77] World Health Organization, Dietary and Inhalation Exposure to nano- and microplastic Particles and Potential Implications For Human Health (2022).
[78] N.A. Yaranal, S. Subbiah, K. Mohanty, Identification, extraction of microplastics from edible salts and its removal from contaminated seawater, Environ. Technol. Innov. 21 (2021) 101253, doi:10.1016/j.eti.2020.101253.
[79] P. Zhou, K. Zhang, T. Zhang, C. Cen, Y. Zheng, Y. Shuai, Release characteristics of small-sized microplastics in bottled drinks using flow cytometry sorting and nile red staining, Water. (Basel) 16 (2024) 1898, doi:10.3390/w16131898.